FACULTY OF SCIENCE AND TECHNOLOGY

MASTER THESIS

Study programme / specialisation:

Environmental engineering/Offshore technology

The spring semester, 2022

Open access

Author: Simen Tungesvik

.....
(signature author)

Course coordinator: Malcolm Kelland

Supervisor(s): Malcolm Kelland

Thesis title: Synthesis and testing of new classes of scale inhibitors

Credits (ECTS): 30

Keywords:
Scale
Scale inhibitors
Moedritzi-Irani
Phosphonates
Environmental regulations
Seawater biodegradability
Calcium compatibility

Pages: 55

+ appendix: 14

Stavanger, 15/06/2022
date/year

Abstract

Scale deposition is a common water related production problem in the oil and gas industry that can lead to damage and reduced production. Scale deposition occurs from sparingly inorganic salts that create an organic precipitate from two incompatible water mixtures. The two most common scales are $CaCO_3$ and $BaSO_4$. Scale inhibitors (SIs) are commonly used to prevent the formation of scale in producing wells. With an increasing demand for more green oilfield chemicals by organisations such as the Oslo-Paris convention (OSPAR), green SIs have become prominent. A common type of SI would be phosphonates. Methylenephosphonate functional groups have been reported to yield efficient scale inhibition and strong adsorption onto the reservoir rock. To get a SI with high biodegradability is difficult, but by phosphonation, the goal was to gain effective scale inhibition and biodegradability by using starting materials claimed to have good biodegradability. The phosphonation of SIs was done via Moedritzi-Irani synthesis where methylenephosphonate groups were attached. Each SI was tested for calcium compatibility, biodegradability by the OECD 306 test in seawater for 28 days, and scale inhibition against calcite and barite scaling on a high-pressure dynamic tube blocking rig. There were two projects, project A and B.

Project A involved synthesis of one, two and three methylenephosphonate groups to tetrasodiumiminodisuccinate (TSIDS) (claimed to have good biodegradability), and the related chemicals tetrasodium ethylenediaminodisuccinate (TSEDAS), and diethylenetriamine Bis-*N*,*N*-Succinic Acid (DETAS), respectively. All synthesized SIs showed poor barite inhibition. Calcium compatibility testing showed excellent results for phosphonated TSEDAS (TSEDAS-P) and moderate for phosphonated TSIDS (TSIDS-P). TSEDAS-P also gave excellent inhibition against calcite scale which would make downhole squeeze treatment a possible option. TSIDS-P showed moderate calcite scale inhibition but precipitated at high concentrations of SI during calcium compatibility testing. This indicated that it was not suitable for squeeze treatment, however, continuous injection topside could be an option if the calcium concentration is moderate to low. TSIDS-P yielded exceptional biodegradability in seawater (OECD306 BOD28: 72.56%) and was considered as readily biodegradable. On the other hand, TSEDAS-P yielded poor seawater biodegradability (2.68%). Phosphonated DETAS (DETAS-P) was only partially soluble as a SI resulting in poor calcite and barite inhibition. No further testing was pursued.

Project B included the phosphonation of glucosamine, a monomer of the natural polymer chitosan. Ball milling was used to synthesize phosphonated glucosamine where results indicated moderate inhibition against calcite scale and poor inhibition against barite scale. Phosphonated glucosamine showed moderate calcium compatibility with only some cloudiness to the solutions when mixing high concentrations. This is not expected to be detrimental for injection as a squeeze treatment. Therefore, the SI could be used for squeeze treatment applications. When tested for seawater biodegradability, the average result was 21% biodegradability.

Contents

Acknowledgements

Firstly, I want to thank Malcolm Kelland for the guidance he has provided throughout the semester. Thank you for providing an interesting, yet challenging masters project.

Thank you to Sumit Ganguly for assistance in the lab and great conversations. Thank you for teaching me how to operate the scale rig and showing me the process for synthesis. He has been fantastic to work with and a great supervisor in the lab.

Thank you to Mohamed Mady for showing me how to operate the ball milling machine and for showing interest in my progression on my projects.

Finally, I want to thank the University of Stavanger for a meaningful and educational time during my master thesis.

List of figures

List of tables

1. Introduction

1.1. What is scale?

Scale formation is the deposition of sparingly inorganic salts from a mixture of two incompatible waters where an organic precipitate is formed. Notably, formation water can become unstable due to changes in reservoir conditions and result in deposition of calcium carbonate ($CaCO_3$) scale. This is the commonest oilfield scale. Also, seawater containing high concentrations of sulphate ions (SO_4^{2-}) can be mixed with produced water containing concentrations of barium ions (Ba^{2+}), calcium ions (Ca^{2+}), and strontium ions (Sr^{2+}) where precipitation of barium sulphate ($BaSO_4$), calcium sulphate ($CaSO_4$), and/or strontium sulphate ($SrSO_4$) will occur. Scale can cause blockage of flow in pipelines, damage to equipment in the well leading to malfunctioning, scale formation in the processing facilities, and limit oil and gas production. Without treatment, scale can grow thick, which is why it must be dealt with early to reduce potential operating costs and halt in production (Binmerdhah & Yassin, 2007; Hasson et al., 2011; Kelland, 2014e; Mady, Malmin, et al., 2019). Scale deposition is one of the most common water-related production problems, along with corrosion and gas hydrates (Kelland, 2014e). Scale deposition in the rock formation can cause reduced porosity and permeability of the formation (Kamal et al., 2018).

1.2. Scale mechanisms

There are two crystallization pathways that form scale, namely, surface crystallization and bulk crystallization. Surface crystallization follows as a result of heterogeneous crystallization of the scale deposits on the pipe surface. Bulk crystallization occurs when crystal particles are formed in the bulk phase through homogeneous crystallization. It may form on pipe surfaces as sediments, forming a layer that can lead to decreased flow. Additionally, supersaturated scale forming conditions will lead to scale growth and agglomeration, which can lead to pipe blockage (Al-Roomi & Hussain, 2016). The general formation of scale has been known to contain four phases. Aggregation, nucleation, crystal growth, and agglomeration (Mpelwa & Tang, 2019).

1.2.1. Aggregation

When the brine system is supersaturated with scaling ions, aggregation occurs. Next, cations (Ca^{2+}) and anions (CO_3^{2-} or SO_4^{2-}) collide to form ion pairs in solution, which form micro-aggregates that act as small centers of crystals or micro-nuclei (Al-Roomi & Hussain, 2016; Kumar et al., 2018; Mpelwa & Tang, 2019).

1.2.2. Nucleation

Some of the newly formed micro-aggregates become nucleation centers for crystallization, which leads to the formation of microcrystals. Nucleation can occur on the substrate and in the fluid bulk at a high ratio of supersaturation (Al-Roomi & Hussain, 2016; Kumar et al., 2018; Mpelwa & Tang, 2019).

1.2.3. Crystal growth

The microcrystals formed will agglomerate and/or absorb into solid surfaces and grow into larger microcrystals. These microcrystals will grow further to form and fuse into macrocrystals (Al-Roomi & Hussain, 2016; Kumar et al., 2018; Mpelwa & Tang, 2019).

1.2.4. Agglomeration

The macrocrystals formed will grow further due to the adsorption of additional scaling ions from solution. This will result in the formation of a scale film on a surface, which will eventually grow into a deposit (Al-Roomi & Hussain, 2016; Kumar et al., 2018; Mpelwa & Tang, 2019).

1.3. Different types of scales

Sandstone formations contain barium and strontium cations, while carbonate formations are comprised of divalent cations such as calcium and magnesium (Adegoke et al., 2021; Frenier & Ziauddin, 2008a, p. 28).

Table 1: List of typical oilfield scales (modified from (Merdhah & Yassin, 2009)).

Name of chemical	Chemical formula	Primary variable
Calcium carbonate	$CaCO_3$	Partial pressure of CO_2, temperature, total dissolved salts, pH
Calcium sulphates: **Gypsum** **Hemihydrate** **Anhydrite**	 $CaSO_4 * 2H_2O$ $CaSO_4 * H_2O$ $CaSO_4$	Temperature, dissolved salts, pressure
Barium sulphate	$BaSO_4$	Temperature, pressure
Strontium sulphate	$SrSO_4$	Temperature, pressure, dissolved salts
Iron compounds: **Ferrous carbonate** **Ferrous Sulfide** **Ferrous Hydroxide** **Ferrous Hydroxide**	 $FeCO_3$ FeS $Fe(OH)_2$ $Fe(OH)_3$	Corrosion, dissolved gases, pH

Table 1 shows typical oilfield scales found, mostly consisting of carbonates and sulphates. Therefore, carbonates and sulphates will be the focus in this thesis as they are commonly associated with problems regarding oilfield scale.

1.3.1. Carbonate scales

There are different types of carbonate scales found in the well area. Some of these include magnesite ($MgCO_3$), Iron (II) carbonate ($FeCO_3$), and $CaCO_3$. Various minerals of $CaCO_3$ exist, namely, aragonite, vaterite, and calcite. Calcite being the most typical (Frenier & Ziauddin, 2008c, p. 28).

1.3.2. $CaCO_3$ scale

$CaCO_3$ is the most common scale found in the topside production facilities and in the upper part of the production tubing. Formation water, which was stable under conditions in the reservoir, can become unstable due to changes in physical conditions such as temperature or pressure prompting $CaCO_3$ scale. $CaCO_3$ scale can also occur due to change in pH and abundance of Ca^{2+} ions and bicarbonate ions in solution (Baker Hughes - Legacy, 2013; Jafar Mazumder, 2020).

Calcium and bicarbonate ions are usually found in produced water. Here, $CaCO_3$ can deposit as a result of the following equilibrium equation shifting to the right:

$$2HCO_3^- \leftrightarrow CO_3^{2-} + H_2O + CO_2 \qquad (1.3.1)$$

When pressure drops during production the equilibrium equation will shift to the right according to the Chatelier's principle to release more CO_2 gas and increase the pressure. However, this will also produce more CO_3^{2-}, which can precipitate $CaCO_3$ if the concentration of CO_3^{2-} ions is high enough. This will lead to the following equation (Chillingar et al., 2008, p. 121; Kelland, 2014h, p. 52):

$$Ca^{2+} + CO_3^{2-} \leftrightarrow CaCO_3 \qquad (1.3.2)$$

The result is a precipitation of $CaCO_3$ as scale deposits.

Factors that can cause the equilibrium of equation 3.1 and 3.2 to shift to the right are: (Chillingar et al., 2008, p. 121):

1. Decrease in pressure.
2. Increase in temperature.
3. Loss of dissolved CO_2.
4. Increase in pH.

1.3.3. Sulphate scale

Group II alkaline earth metal ions, apart from magnesium, can form sulphate scales by reacting divalent metal ions with sulphate ions as described in the equation below (Kelland, 2014h, p. 53):

$$M^{2+} + SO_4^{2-} \rightarrow MSO_{4(s)} \qquad (1.3.3)$$

Sulphate scales are commonly found where seawater injection applications are present. Sulphate scale deposits occurs due to a mixing of injected seawater containing high concentrations of SO_4^{2-} ions with low concentrations of Ba^{2+}, Ca^{2+}, and Sr^{2+} ions. This seawater will mix with the formation water in the reservoir containing high concentrations of Ba^{2+}, Ca^{2+}, and Sr^{2+} ions, with low concentrations of SO_4^{2-} ions. This mixture creates sulphate scales such as $BaSO_4$, $CaSO_4$, and $SrSO_4$. Calcium sulphate can occur in three separate crystalline forms

such as $CaSO_4 \bullet 2H_2O$ (gypsum), $CaSO_4 \bullet \frac{1}{2}H_2O$ (calcium sulphate hemihydrate), and $CaSO_4$ (calcium sulphate anhydrite) (Chillingar et al., 2008; Kamal et al., 2018; Merdhah & Yassin, 2009).

Sulphate scales are difficult scales to remove due to low solubility. Sulphate scales with a high K_{sp} in solution have higher solubility. Of all sulphate scales, barium sulphate has the lowest K_{sp} of about $10^{-9.99}$ at 25°C and is the least soluble in solution. The solubilities of different sulphates can be seen in Figure 1 (Jafar Mazumder, 2020).

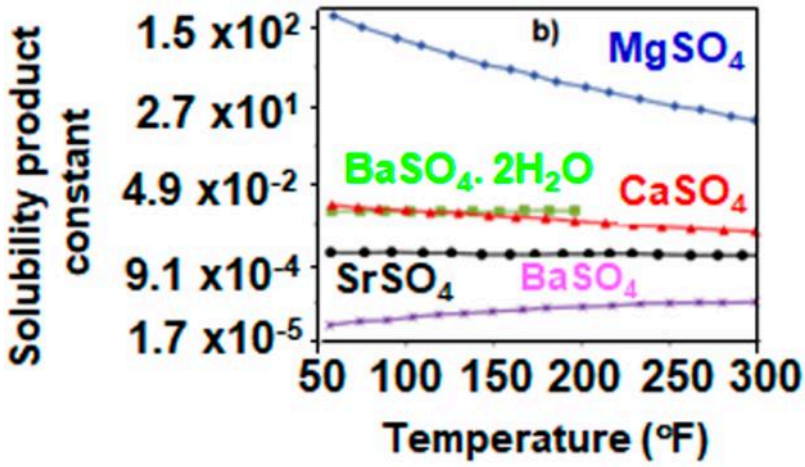

Figure 1: Solubility of sulphate scale with increasing temperature (Jafar Mazumder, 2020).

1.3.4. $BaSO_4$ scale

Barium sulphate is a difficult sulphate scale to control as a result of its low solubility (Kelland, 2014h, p. 53). Barium sulphate can be obtained from two primary sources. The first, and main one, being from the injected seawater where SO_4^{2-} ions react with Ba^{2+} ions in the formation to form barite scale deposition. The second source is from drilling operations where barite is used as a weighting material. During these operations, the invasion of the mud filtrate will create a mud cake due to the pressure difference. This mud cake contains mostly barite where the barite particles can invade into the formation resulting in barite scale. This can block pores in the formation, leading to reduced permeability (Bageri et al., 2017). In this thesis, the focus will be on the injected seawater, which result in $BaSO_4$ deposition due to an excess amount of SO_4^{2-} and Ba^{2+} ions in the zone of injection (Jafar Mazumder, 2020). The amount of scale deposited is also depended on temperature where higher temperatures result in more scale formed (Frenier & Ziauddin, 2008c, p. 36).

1.4. Treatment methods

There are different ways to treat scale deposition formed during production that all vary in cost, efficiency, and environmental impact. There are mechanical and chemical scale removal methods, but the most common method is by preventing scale formation using scale inhibitors (SIs).

1.4.1. Mechanical scale removal

Mechanical removal of scale has previously been used by drilling or reaming. However, this method of removing scale is very expensive since a drilling rig must be brought in for the process. Further, the drilling rig can have problems reaching deep wells. Another factor to consider is that the well is not re-stimulated, as drilling does not remove the scale deposits from the formations. These scale deposits can cause formation damage leading to a decrease in production. Therefore, drilling is only considered as a last option for scale removal, and chemical methods are generally preferred (Olajire, 2015).

1.4.2. Chemical scale removal

Carbonate scales such as $CaCO_3$ scale can be removed using chemical methods. $CaCO_3$ can be dissolved using acids such as hydrochloric acid (HCl), which is a cheap option (Fink, 2021a). However, HCl needs an additive such as a corrosion inhibitor to prevent sludge precipitation from happening (Kelland, 2014a).

$$2HCl + CO_3^{2-} \rightarrow H_2O + CO_2 + 2Cl^- \qquad (1.4.1)$$

Additionally, HCl is not environmentally friendly as it is toxic and highly corrosive (Kamal et al., 2018). Another way to chemically dissolve scale would be using ethylenediaminetetraacetic acid (EDTA). As opposed to HCl, EDTA is non-toxic, however, the biodegradation rate is low. It has been used as a scale dissolver to remove both carbonate and sulphate scale (Almubarak et al., 2017; Fink, 2021a; Shaughnessy & Kline, 1983).

1.5. Scale inhibitors

SIs are chemical agents used to reduce the rate of formation of a fouling scale on a surface in water systems, and the use of SIs is common to combat various types of scales (Frenier & Ziauddin, 2008b; Kamal et al., 2018). To prevent scale deposition, SIs are used to treat the well area that has scale forming in the nearby wellbore. SIs are chemicals added to the brine to prevent the formation of scale in a reservoir (Jafar Mazumder, 2020). They are commonly used in the oil and gas industry where the most common types of scales are $CaCO_3$ and $BaSO_4$. There are physical and chemical methods to prevent scale. Some examples of these methods include pH control, ensuring that two incompatible waters do not mix, reduction of supersaturation by initiating scale formation, reducing sulphate ions in the injected seawater, diluting the produced water, and membrane filtration to reduce sulphate in injection water. The most used SIs are added in water in the area where the crystals would start to form. This means that the SI must be added in the upstream of where the scale crystals will form. To ensure crystal growth inhibition, the SI must be present in the water continuously to ensure that no new scale crystals are formed. This can be achieved through continuous chemical injection or using the squeeze treatment method (Kan et al., 2020).

Phosphorous based SIs are often used due to their high inhibition performance, although these SIs can be toxic. Further, eutrophication problems can occur if high concentrations of phosphorous are released into the surrounding environment of an oilfield. Therefore, it is important to limit the amount of phosphorous concentration used in SIs (Jafar Mazumder, 2020).

Some important ions attached to organic molecules that work well as SIs are (Kelland, 2014f, p. 57):

- Phosphate ions ($-OPO_3H^-$)
- Phosphonate ions ($-PO_3H^-$)
- Phosphinate ions ($-PO_2H^-$)
- Carboxylate ions ($-COO^-$)
- Sulfonate ions ($-SO_3^-$)

These active functional groups aid in inhibiting crystal growth by binding strongly or weakly to the divalent cations in the formations, with the forming nuclei, or the growing crystal. By preventing crystal growth, SIs work to retard the scale formation in a producing system (Jafar Mazumder, 2020). Functional groups are discussed further in chapters 1.5.4 and 1.5.5.

1.5.1. Batch treatment

During a batch treatment, a certain volume of SI is injected into the processing facility at a regular interval. Here, the goal is to have the SI adsorb onto the reservoir surface where the SI will be retained. However, this process requires the well to be closed before resuming production, and SI can be wasted if it is not retained well (Adegoke et al., 2021; Zhang et al., 2019).

1.5.2. Continuous injection

Continuous injection is the constant injection of SI using injection lines either topside or downhole (Kelland, 2014d, p. 72). This method can be recommended in wells that do not need to be squeezed due to low scaling potential in the near wellbore. Continuous injection can also be an option if squeeze treatment is costly or difficult to perform regularly. However, the quantity of SI used is far greater than for batch treatment and setup and installation can be costly (Adegoke et al., 2021; Hustad et al., 2012).

1.5.3. Squeeze treatment

A widely used method to add a SI downhole is using the SI squeeze treatment. This method can be used to inject SIs where the conditions are harsh such as in a high-pressure high-temperature (HPHT) well or where Ca^{2+} concentrations are high (Kelland, 2014g, p. 75). A squeeze treatment involves an injection (usually a batch injection) of SI into a producing formation where it will prevent scale deposition. Here, the concentration of SI must be above the minimum inhibitor concentration (MIC) to effectively inhibit scale in the formations (Kan et al., 2020; Vazquez et al., 2016). An illustration of the squeeze treatment method can be seen in Figure 2.

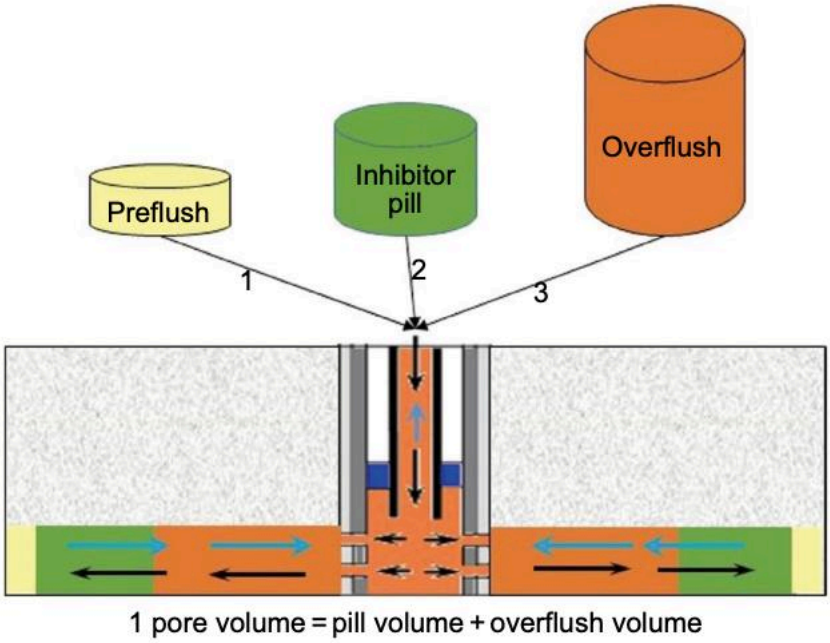

Figure 2: Sale inhibitor squeeze treatment illustration (modified from (Kan et al., 2020)).

Firstly, a squeeze treatment begins with a preflush of a small volume of chemical injected into the well to clean the production tubing and act as a buffer (Kan et al., 2020; Vazquez et al., 2016). Typical chemicals used here would be surfactants, acids, and biocides. Next, the SI is injected and pushed down into the formation. The SI usually contains 0.5-10% (w/v) in makeup water of either about 1% KCl solution or produced water that has been filtered. Further, a new volume of fluid is injected, which will displace the SI further down into the formation. This addition of fluid is called the overflush (Kan et al., 2020). Finally, there is a shut-in stage where the chemical SI can be retained further in the formation at a high level (Vazquez et al., 2016). When production is put back on after shut-in, produced water will flow and dissolve some of the retained SI. Further, the produced water containing some SI will be able to prevent scale deposition (Kelland, 2014g, p. 72). Effective SIs have low MICs, allowing for increased squeeze lifetimes. The squeeze lifetime of a SI is the amount of time until the concentration of SI falls below the MIC and a resqueeze is needed (Tantayakom et al., 2005; Zotzmann et al., 2018). Phosphorous atoms are commonly used to track the SI concentration to ensure the concentration stays above the MIC. Phosphorous is one of the more accurate methods to track, however, there are other alternatives to monitor the MIC without phosphorous such as scanning electron microscopy, stressed tests, and in-line monitoring (Kelland, 2014g, p. 73; Mady, Fevang, et al., 2019). Typical values for MIC are usually between 1-20 ppm. Therefore, a longer squeeze lifetime will ensure that SI chemicals will have to be injected less frequent making it cost efficient (Tantayakom et al., 2005). Squeeze lifetime is also extended by longer retention times. Retention time is the amount of time the SI can adsorb onto the porous media after being deployed. Efficient adsorption capabilities result in longer squeeze lifetimes and keeps the SI concentration above the MIC for longer durations of time (Adegoke et al., 2021; Jarrahian et al., 2019).

1.5.3.1. Precipitation squeeze

Another method to deploy a SIs would be by the precipitation squeeze method. SI squeeze treatments can result in interactions between the SI and carbonate mineral substrates leading to

a SI/Ca complex. This precipitation can be a controlled precipitate, which is the precipitation squeeze method (Jarrahian et al., 2019). Precipitation squeeze involves injecting the SI into the formation followed by a shut off in production where the SI reacts with the divalent cations in the formation (or other injected cations) to form an insoluble salt which will precipitate in the pores of the rock formations (Fink, 2021a; Tantayakom et al., 2005). An example would be using an acidic phosphonate SI pill that would precipitate calcium phosphonate into the formations after injection (Kan et al., 2020). This has been a successful method to utilize SIs to combat inorganic scale. However, some of the downsides with precipitation squeeze treatment occurs when the SI is only retained in the formations for short periods of time, resulting in lower treatment lifetime (Tantayakom et al., 2005). A method to increase the SI retention time using precipitation squeeze is by increasing the pH of the SI in solution in situ near the wellbore area. This ensures that the anionic form from the acid groups in the inhibitor molecule, will react with the cations (Ca^{2+}, Mg^{2+}, etc.) to create a complex that will precipitate out. An example would be to add urea to the SI solution where high temperatures in the formations will cause urea to react and produce ammonia as seen below. Ammonia is a basic gas and will increase the pH of the SI solution resulting in more complexes being made between cations (Ca^{2+} and Mg^{2+}) and anions. However, urea only breaks down above 85°C, which means that urea cannot be utilized in low temperature wells alone (Kelland, 2014g, p. 75).

$$NH_2CONH_2 + H_2O + heat \rightarrow 2NH_3 + CO_2 \qquad (1.5.1)$$

Currently, precipitation squeeze treatments are used less often than adsorption squeeze treatments due to the possibility of blocking of formations and damage to the wellbore region as a result of inhibitor precipitation (Tantayakom et al., 2005).

1.5.3.2. Adsorption squeeze

The adsorption/desorption features of a SI can extend the scale squeeze lifetime and improve the efficiency of the SI. The adsorption of a SI takes place on the reservoir rock and then slowly desorbs by fluid removal (Khormali et al., 2017). The mechanism of adsorption of SI occurs through wan der Waals and electrostatic interactions between the formation minerals and the SI. In this process polymers (or phosphonates) can be described by an adsorption isotherm denoted Γ(C). Here, Γ(C) is a function of pH, cation concentration, mineral substrate, temperature, and molecular weight. Also, by determining the exact form of Γ(C), the squeeze lifetime will be determined (Jordan, Sorbie, Griffin, et al., 1995). The optimal features of adsorption/desorption of a SI include a large volume of reagent to adsorb on the rock followed by a slow desorption of the SI off the rock. This results in an extended squeeze lifetime and efficient inhibition of scale deposition (Khormali et al., 2017).

A study by Jordan et al. (1995) was conducted using polyphosphino carboxylic acid (PPCA) and diethylene triamine penta (methylene phosphonic acid) (DETPMP) as SIs for static adsorption in different reservoirs. Tests showed that the higher levels of bulk adsorption on the reservoir rock resulted in increased lifetime. However, due to the different natures and conditions of reservoirs, there cannot be drawn any direct conclusion regarding adsorption effect on scale squeeze lifetime (Jordan, Sorbie, Yuan, et al., 1995).

1.5.4. Commercial scale inhibitors

In recent decades, functional groups such as phosphonates, carboxylic acids, and sulfonic acids have proven to be effective for scale inhibition. Common commercial SIs often contain some of these functional groups (Ji et al., 2017).

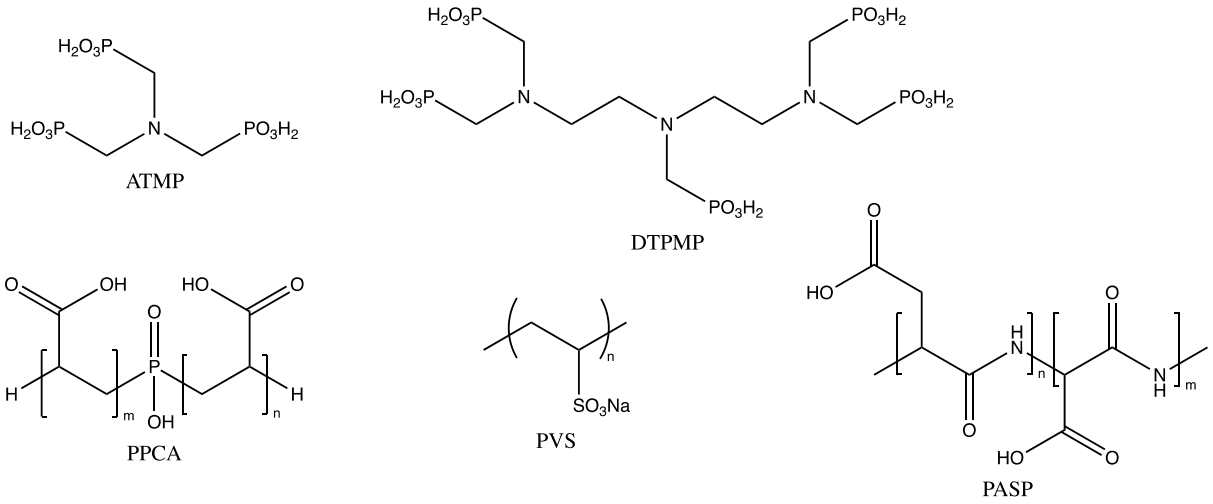

Figure 3: Structures of commercial SIs (Aminotriss(methylenephosphonic acid), Diethylenetriamine penta(methylene phosphonic acid), Polyphosphino carboxylic acid, Polyvinylsulfonate, and Polyaspartic acid (Adapted from (Fink, 2021b; Kelland, 2014f, p. 64; Mady et al., 2022; Veisi et al., 2019; Zeng et al., 2013)).

Figure 3 shows some examples of commercial SIs containing phosphonate (ATMP, DTPMP), sulfonate (PVS), and carboxylate (PPCA, PASP) functional groups.

ATMP is a commercial SI containing three phosphonate functional groups, and has been reported to inhibit $CaCO_3$ scale efficiently (Ji et al., 2017). Polyaspartic acid (PASP) is considered an efficient SI against both carbonate and sulphate scale. It is phosphate-free with low toxicity and high biodegradation, therefore, making it environmentally friendly. (Liu et al., 2011) PVS is a known commercial sulfonate SI that prevents carbonate and sulphate (particularly $BaSO_4$) scale. PVS is typically injected into the producing well during a squeeze treatment, but it suffers from poor adsorption onto the reservoir rock formation. This results in a poor squeeze lifetime in the reservoir (Veisi et al., 2019).

Typical SIs need to have certain properties that can make for effective scale inhibition. SIs that are thermally stable can be used in squeeze treatments in HTHP wells. Here, the SI can withstand temperatures higher than 160°C. SIs used in these harsh environments that are not thermally stable can be exposed to thermal degrading. Here, hydrolysis can destroy the part of the molecule that would bind to the scale lattice, such as a functional group (Graham et al., 1997). In general, the functional group of a SI can aid in effective adsorption onto the reservoir rock, allowing for the SI to achieve longer squeeze lifetimes.

1.5.5. Phosphonates

Phosphonate SIs show great inhibition for mineral scale formation, preventing both calcite and barite scales in oil and gas production systems (Tomson et al., 2003). The phosphonate functional group (-PO_3H_2) is common in many commercial SIs such as ATMP and DTPMP (Figure 3). ATMP and DTPMP are both non-polymeric aminophosphonated compounds that

display exceptional inhibition against carbonate and sulphate scales under harsh conditions (Mady et al., 2022).

Previously based studies have specified that most amine methylene phosphonic acid-based inhibitors were generally considered as not thermally stable compared to polymeric species such as PVS. Therefore, they are not usually recommended for squeeze treatment in HPHT wells of temperatures above 160°C (Fink, 2021b; Graham et al., 1997). However, recent studies have reported that most aminophosphonated SIs are thermally stable and can extend squeeze lifetimes (Mady et al., 2022). The amine group in aminomethylenephosphonates also allow for greater inhibition by an increased chelating effect on scaling cations. Another advantage of phosphonates include increased squeeze lifetimes through strong adsorption onto the reservoir rock (Mady, Fevang, et al., 2019). Additionally, phosphonates have been shown to not hydrolyze easily, especially at high temperatures (121.1°C) where oxygen is absent (Fink, 2021b). Some amine methylene based phosphonate SIs have proven to be thermally stable above 160°C (Graham et al., 2000). A study by Dyer et al. (2004) tested the thermal stability of HMDP (hexamethlenediamine tetramethylene phosphonic acid), NTP (nitrilotris methylene phosphonic acid), and HMTPMP (bis (hexamethylene) triaminepentakis (methylene phosphonic acid)) using thermal ageing (160°C) after testing the SIs against carbonate and sulphate scale. The results showed great scale inhibition against carbonate scale after thermal ageing, but inhibition against sulphate scale was reduced.

1.6. Environmental regulations

Produced water discharge from oilfields can contain hazardous chemicals and residual oil that can be dangerous to the environment (Kelland, 2014c). Therefore, rules and regulations are set in place to prevent such hazardous discharge. In Norway, the Oslo-Paris (OSPAR) convention decides the regulations and classification of oilfield chemicals for discharge (Norwegian oil and gas association, 2017). The different classifications for these oilfield chemicals are showcased in Table 2.

Table 2: Table for classifying and reporting chemicals. Modified from (Norwegian oil and gas association, 2017).

<table>
<tr><th colspan="2">Environmentally friendly/Acceptable</th><th colspan="2">Not environmentally acceptable</th></tr>
<tr><td>Green</td><td>Yellow</td><td>Red (should be replaced)</td><td>Black (prohibited)</td></tr>
<tr><td rowspan="4">PLONOR list</td><td>Biodegradability >60%
Log Pow ≤ 3, or toxicity EC_{50}/LC_{50} ≤ 10mg/l</td><td>Two of three categories: Biodegradability <60%, log Pow ≤ 3, or toxicity EC_{50}/LC_{50} ≤ 10mg/l</td><td>Biodegradability <20% and log Pow > 5</td></tr>
<tr><td rowspan="3">Biodegradability 20-60%
log Pow ≤ 3, or toxicity EC_{50}/LC_{50} ≤ 10mg/l</td><td>Biodegradability <20%</td><td>Biodegradability <20% and toxicity EC_{50}/LC_{50} ≤ 10mg/l</td></tr>
<tr><td>Inorganic and toxicity EC_{50}/LC_{50} ≤ 1mg/l</td><td>Hazardous to reproduction, hormones, or genes, etc.</td></tr>
<tr><td></td><td>No test data</td></tr>
</table>

Oilfield production chemicals are sectioned into four different categories (green, yellow, red, black) based on the properties of the chemical. Green and yellow chemicals are considered environmentally friendly and show high biodegradability, low toxicity, and low bioaccumulation (Norwegian oil and gas association, 2017). According to the OSPAR convention there are criteria that need to be satisfied for a polymer to be biodegradable. These criteria include Over 60% biodegradation within 28 days, a toxicity of LC_{50} or EC_{50} to be > 1mg/L for inorganic species and LC_{50} or EC_{50} > 10mg/L for inorganic species, and lastly, a bioaccumulation of log (P_{OW}) < 3. A chemical can be listed on the pose little or no risk (PLONOR) list if two or three of these criteria listed are achieved and the chemical has a biodegradability > 20% within 28 days in seawater (Hasson et al., 2011). To test biodegradability the organization of economic cooperation and development (OECD) 306 seawater test is used which shows how a material biodegrades in seawater (Almubarak et al., 2017; Ott et al., 2019). Red and black chemicals are labeled as not environmentally friendly and should be replaced or are prohibited from use (Norwegian oil and gas association, 2017).

1.7. Green scale inhibitors

The growing concern regarding hazardous discharge from oilfield chemicals has led to more researchers developing greener SIs (Jafar Mazumder, 2020). By taking the OSPAR regulations as the standard, there are three main factors to consider for green SIs. These factors include the rate of biodegradation, toxicity, and bioaccumulation. SIs must be water soluble to inhibit through water, which means the bioaccumulation will be low as well (Kelland, 2014b). Toxicity is also difficult to modify as this depends on the SI. Some factors to reduce toxicity would be high molecular weight (>1000), reduce water solubility (<1µg/L), and increasing steric hindrance at active sites (Boethling et al., 2007). Polymers and non-ionic surfactants have generally low toxicity, although cationic surfactants and polymers can be more toxic. Therefore, the rate of biodegradation is the simplest factor to affect (Kelland, 2014b). Biodegradation is the rate of degradation by microorganisms. For SIs this occurs in seawater where there are less bacteria exposed to chemicals compared to freshwater (Kelland, 2014b).

As previously mentioned, many green chemicals are non-toxic and non-bioaccumulative, which puts a great emphasis on biodegradability. An example would be the use of phosphonates which are commonly non-bioaccumulative and non-toxic. However, phosphonates usually have poor biodegradability. Ideally, the biodegradability of a green SI should be >20%, but the most optimal would be >60-70%. Still, high biodegradation is difficult to achieve, but there are certain molecular features that can increase the rate of biodegradation. These include groups subject to enzymatic hydrolysis (mainly esters and amines), oxygen atoms in the form of hydroxyl, aldehyde, or carboxylic acid groups, and unsubstituted linear alkyl chains and phenyl rings (Boethling et al., 2007).

Still, biodegradable SIs have accompanying challenges that follow. Green biodegradable SIs usually have poor thermal stability with poor performance in harsh conditions (Kelland, 2014b). Also, low inhibition performance and poor adsorption abilities can lower the efficiency of the SI. Therefore, highly efficient green SIs are difficult to synthesize. Nonetheless, green SIs are mostly renewable, biodegradable, and ecologically acceptable, which are prominent features when following environmental regulations (Jafar Mazumder, 2020).

1.8. Project relevancy

With an increasing focus on more environmentally friendly solutions to scale prevention, this thesis includes work to synthesize new biodegradable SIs. Lab tests were performed where SIs with phosphonate functional groups were synthesized using the Moedritzi-Irani reaction. By following the regulation for "green" SIs set by the OSPAR convention, the lab work done in the thesis focuses on making efficient SIs that are biodegradable. Project A involves phosphonating water-based chemicals to achieve efficient scale inhibition and higher biodegradation. Project B is based on a paper by Mady *et al.* (2021) on phosphonated chitosan. Here, the goal is to phosphonate glucosamine, a monomer of the natural polymer chitosan, to investigate the efficiency of the SI performance and biodegradability.

2. Materials and methods

2.1. Chemicals

All starting materials and solvents used to synthesize SIs in this thesis were purchased from Bayer (Lanxess), VWR, and Sigma-Aldrich (Merck). All chemicals were used without further purification.

2.2. Characterization of oilfield scale inhibitors

Nuclear magnetic resonance (NMR) spectroscopy was used to characterize the SI products and verify the reaction. Two to three drops of D_2O were added to about 0.5 mL of SI before the NMR spectra was recorded on a 400 MHz Bruker NMR spectrometer in D_2O. ^{31}P NMR and ^{1}H NMR were also recorded in D_2O (Mady et al., 2016).

2.3. Moedritzi-Irani synthesis

The Moedritzi-Irani reaction allows for the attachment of methylenephosphonate functional groups to aminomethylenephosphonic acids. Here, methylenephosphonates attach to primary and secondary amines. The use of formaldehyde (HCHO), phosphorous acid (H_3PO_3), and catalytic HCl performs the attachment of a methylenephosphonate to an amine by conventional conditions (Mady & Kelland, 2017). The following procedure for the synthesis of oilfield SIs using Moedritzi-Irani is based on a paper by Mady *et al.* (2019).

First, the base chemical (TSIDS, 2.00g) was added to a 100 mL round bottom Erlenmeyer flask containing a second funnel. Next, 15 mL of deionized water was measured where 13 mL was added along with a magnetic stirrer. Then, H_3PO_3 (1.2 mol equivalents) was dissolved with the remaining 2 mL deionized water using a spatula. The dissolved H_3PO_3 was added dropwise to the solution. Subsequently, HCl (37 wt %, 6 mol equivalents), was added to the solution, dropwise. Afterward, the flask was heated to about 63°C in an oil bath and connected to a condenser with a water inlet and outlet, creating a reflux (Figure 4). As the solution was heating up, a nitrogen balloon was prepared and attached at the top of the condenser. Next, aqueous HCHO (37 wt %, 1.5 mol equivalents) was added dropwise using a syringe. The solution was left to mix for about two minutes before the temperature was raised to 115°C. After reaching this temperature, the solution was left to reflux for 24 hours with vigorous stirring. After 24 hours of reflux, the solution was neutralized to pH 6-7 by dropwise addition of sodium hydroxide (NaOH) (20%, 1 mol equivalents).

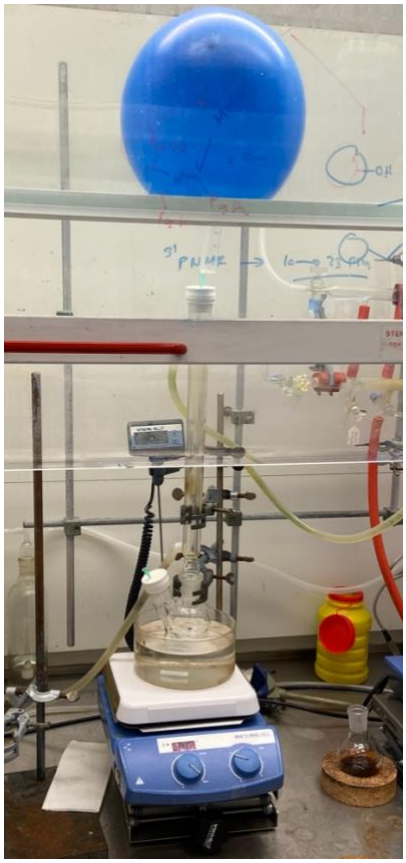

Figure 4: Reflux setup with condenser in oil bath.

2.4. Ball-Milling method

When conventional Moedritzi-Irani using reflux yielded poor results, ball milling was used. This method synthesizes Moedritzi-Irani using only solid components and a small amount of deionized water. Figure 5 shows the setup used for ball milling.

Figure 5: Planetary micro mill Pulverisette 7 classic line ball mill.

Firstly, the starting compound (glucosamine, 1.00g) was mixed with H_3PO_3 (2 mol equivalents) and paraformaldehyde (P(HCHO)) (2 mol equivalents) before being placed in a zirconium (IV) oxide (ZnO_2) bowl. Then, 70g of zirconium oxide grinding balls (diameter=3mm Ø) were added to the bowl. A small volume of deionized water (0.5 mL) was also added to the bowl to increase mixing. The bowl was then placed in a planetary micro mill Pulverisette 7 classic line ball mill together with a second (empty) bowl for stabilization. Programming operations were set to 750 rpm for 8 hours (20 min runtime, 1 min cooldown period, 24 repetitions). After milling, the solution mixture was set to cool and later filtrated using a strainer. Deionized water was used to filter the solution mixture, separating it from the zirconium oxide balls. Next, the solution was dried under vacuum using a rotary evaporator, resulting in a dried powder.

2.5. High-pressure dynamic tube blocking rig

SI performance testing was executed using a high-pressure dynamic tube blocking rig (build by Scaled Solutions Ltd., Scotland, U.K.) (Figure 6). The rig simulates the conditions in a producing line downhole. Results from tests using the rig gives estimated MIC values for the SI. Tests were made from SI concentrations with values ranging from 1-100 ppm. However, optimal values for SI performance would often be between 1-5 ppm. For our experiments, $CaCO_3$ and $BaSO_4$ scales were evaluated using the rig. The procedure and description of the scale rig used in this thesis is based on a paper by Mady *et al.* (2020).

Figure 6: Front view of High-Pressure dynamic tube blocking rig (from left: pump 1, pump 2, pump 3).

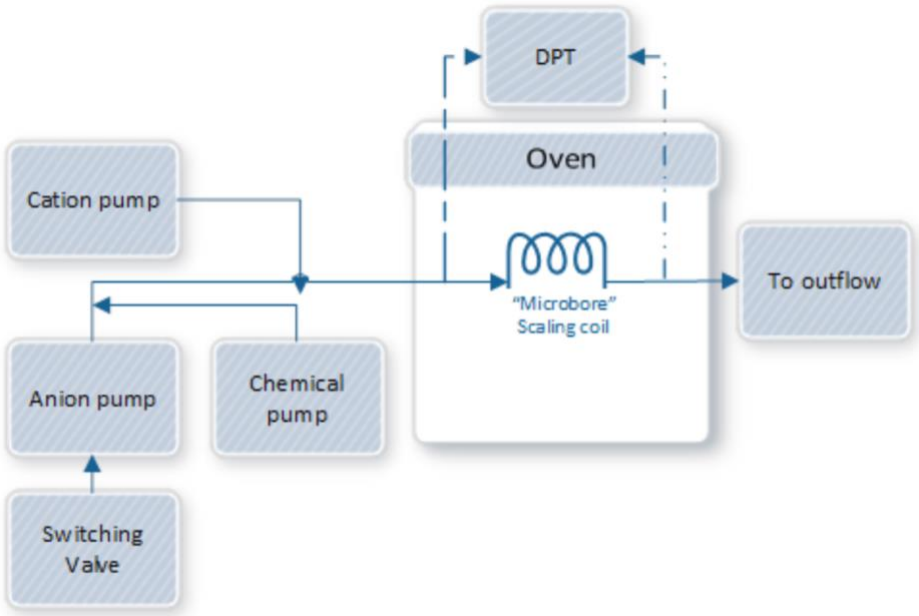

Figure 7: Schematic diagram of the high-pressure dynamic tube blocking rig (Mady et al., 2020).

Figure 7 shows a schematic diagram of the high-pressure dynamic tube blocking rig displaying the different components. Here, the main section of the rig contains three pumps that can pump fluid at a rate of 10 mL/min through a 316 micro bore coil. The coil has an inner diameter of 1mm, a length of 3 meters and is placed in the oven at 100°C. The pressure in the tube was at 80 bar. Three pumps are connected to the rig, labelled 1, 2, and 3 respectively (Figure 6). Pump

1 (cation pump) contains brine 1 injecting scaling cations, pump 2 (anion pump) contains brine 2, which injects the scaling anions, and pump 3 (chemical pump) contains the injected SI. The rig can tolerate temperatures up to 200°C and pressures up to about 4200 psi (300 bar) (Mady et al., 2020).

In this experiment, there were four stages of testing.

1. A blank test only combining brine 1 and 2 without SI.
2. Testing with scale inhibitor pumped in at decreasing concentrations every hour. First dose being at 100 ppm followed by 50 ppm, 20 ppm, 10 ppm, 5 ppm, 2 ppm, and 1 ppm.
3. A repetition of the test SI starting automatically after the previous concentration led to scale formation. This repeat test of SI starts with the concentration of one before scale formation was formed in the previous test.
4. Another blank test with only brine 1 and 2 without SI.

The difference in pressure across the coil is measured along with the rate of scaling and from this, initiations are made. The scale rig is connected to a computer where the results are stored in an excel file. Further, excel is used to plot the data acquired from the tests. The test results show the failed inhibitor concentration (FIC), which occurs when the differential pressure exceeds 14 psi. Additionally, a washing procedure was initiated between each stage of testing. The wash consisted of 10 minutes of EDTA (pH=12-13) being pumped at 9.99 mL/min followed by 10 minutes of distilled water at 9.99 mL/min and finally 2 seconds of anion brine at 9.99 mL/min to complete the wash (Mady et al., 2020).

2.5.1. Composition of brine fluids

The compositions of brine fluids were modeled after production from the Heidrun oilfield, Norway. The composition of aqueous produced fluids used are shown in Table 3. $CaCO_3$ scaling was made using only formation water, and barium sulphate scaling was made using a 50/50 mixture of formation water and the simulated seawater. The necessary amount of salts for carbonate (Table 4) and sulphate (Table 5) brines were dissolved in deionized water. Next, the brine solutions were mixed using a magnetic stirrer, while simultaneously being degassed using a vacuum pump for 15-20 min. Degassing was necessary to remove any gas bubbles that could disrupt the flow of injected brine during testing on the rig. Note that sodium bicarbonate ($NaHCO_3$) was added after degassing of brine 2 to avoid interference with the equilibrium between $NaHCO_3$ and dissolved CO_2 (Jensen & Kelland, 2012; Kelland, 2011).

Table 3: Composition of Heidrun, formation water, seawater, and a 50/50 mixture.

Ion	Heidrun formation water (ppm)	Seawater (ppm)	50/50 Mixed brine (ppm)
Na^+	19510	10890	15200
Ca^{2+}	1020	428	724
Mg^{2+}	265	1368	816.5
K^+	545	460	502.5
Ba^{2+}	285	0	142.5
Sr^{2+}	145	0	72.5
SO_4^{2-}	0	2960	1480
HCO_3^-	880	120	500

Table 4: Salts used to make brine 1 and 2 for carbonate scaling.

Ion	ppm	Chemical formula	g/L	g/3L	g/5L
Na^+	19510	NaCl	49.59	148.77	247.97
Ca^{2+}	2040	$CaCl_2*2H_2O$	7.48	22.45	37.42
Mg^{2+}	530	$MgCl_2*6H_2O$	4.43	13.30	22.16
K^+	1090	KCl	2.0781	6.23	10.39
Ba^{2+}	570	$BaCl_2*2H_2O$	1.0138	3.04	5.07
Sr^{2+}	290	$SrCl_2**6H_2O$	0.8824	2.65	4.4122
HCO_3^-	2000	$NaHCO_3$	2.76	8.26	13.76

Table 5: Salts used to make brine 1 and 2 for sulphate scaling.

Ion	Ppm	Chemical formula	g/L	g/3L	g/5L
Na^+	19510	NaCl	38.64	115.92	193.20
Ca^{2+}	2040	$CaCl_2*2H_2O$	5.31	15.93	26.55
Mg^{2+}	530	$MgCl_2*6H_2O$	13.66	40.98	68.30
K^+	1090	KCl	1.9200	5.76	9.60
Br^{2+}	570	$BaCl_2*2H_2O$	0.5100	1.53	2.55
Sr^{2+}	290	$SrCl_2**6H_2O$	0.4400	1.32	2.2000
SO_4^{2-}	2960	Na_2SO_4 Anhydrous	4.38	13.14	175.20

2.6. Seawater biodegradability test

Biodegradation is the transformation of a chemical as a result of biological activity. The chemical is used by microorganisms to produce new energy as biomass. To understand the fate of a chemical in the environment, the biodegradability of a chemical can be tested. Biodegradability testing of SIs allow for a comprehension of the persistence of a chemical in an aquatic environment. A chemical that degrades quickly is considered "readily biodegradable", and "persistent chemicals" will degrade slowly. Therefore, biodegradability testing of SIs plays an important role concerning discharge offshore. Here, readily biodegradable SIs will not pose long term ecological damage to the environment, unlike persistent chemicals (Mady, Malmin, et al., 2019; Wennberg et al., 2017).

Seawater biodegradability testing is done for oilfield SIs where a common testing method is OECD 306. As mentioned in 1.6, oilfield SIs need to achieve a biodegradability > 20% to avoid being classified as a red or black chemicals (Wennberg et al., 2017). For this thesis, the OECD 306 method was used where the biological oxygen demand (BOD) was measured using the OxiTop Control manometric system (WTW, Germany). The test lasted for 28 days. All the test flasks used contained seawater, nutrients, and the test chemical. Test chemicals prepared for the OECD 306 test were 1% solutions of SIs and their starting material in 10 mL bottles (Appendix A, 0). There were three types of control flasks made. Firstly, blanks containing

seawater and nutrients only, which acted as a base line. Secondly, negative controls containing nutrients, autoclaved seawater, and the test chemical with a final concentration of 69 mg/L. Lastly, positive controls with seawater, nutrients, and sodium benzoate (readily biodegradable substrate) at 100 mg/L. The positive and negative controls were used to reduce the occurrence of false positive and negative controls. In the end, the percent biodegradability was calculated by comparison of the BOD and the calculated theoretical oxygen demand (ThOD). The OECD 306 tests were carried out by Hong Lin (lab engineer) (Mady, Malmin, et al., 2019).

The procedure for the OECD 306 tests was based on a paper by Mady *et al.* (2019). First, the seawater needed for the tests was collected from Mekjarvik (Near Stavanger, Norway) at NORCE research station. The collected seawater was kept in a dark room at 20°C overnight before being transferred to 510 mL amber bottles the next day. The OxiTop was made ready before different nutrients were added to the amber bottles along with measuring heads. Subsequently, the bottles were incubated for 3 hours at 20°C. After incubation, 1.8 mL of a 1% (w/w) solution of each test chemical was added to the test and to the negative control flask. The positive control flask contained 1.0 mL of a 30 g/L sodium benzoate solution. Next, the amber bottles were capped with measuring heads containing NaOH pellets to remove CO_2. The bottles were placed on magnetic stirrers in an incubation cabinet. Data collection was begun instantly. Oxygen consumption was recorded over the 28 days of testing. Thereafter, the data was downloaded to the bottle heads and the ThOD was calculated for the SI before being classified in the OECD guidelines. Complete nitrification was accounted for. Before determining the percent biodegradability, blank oxygen values (BOD values representing background respiration in seawater) were subtracted from the BOD of each test.

2.7. Calcium compatibility test

Calcium compatibility tests were made to clarify that the SI is compatible with Ca^{2+} ions. The test would show if the SI created a complex (SI-Ca) where precipitate was formed, or if there was no complex and the solution was clear. Also, if the SI would be used for squeeze treatment, the calcium compatibility must be excellent as precipitation can lead to formation damage. This is also applicable for reservoirs that contain high concentrations of calcium brines (Mady, Malmin, et al., 2019). The calcium compatibility tests were performed by following the procedure below.

First, a stock solution of 30000 ppm NaCl (3wt%) was prepared. Next, three bottles of Ca^{2+} dosages (100, 1000, and 10000 ppm) were dissolved with 80 mL NaCl solution. Next, four bottles of scale inhibitor dosages (100, 1000, 10000, 50000 ppm) were dissolved with 30 mL NaCl solution. Afterwards, each concentration of SI was mixed with each concentration of Ca^{2+} in a total of 12 glass bottles. The pH was adjusted to be between 4.1 and 4.3 for each bottle and the lids were closed tight. Finally, the bottles were put in an oven at 80°C for 24 hours. The bottles were inspected on initial mixing, after 30 minutes, 1 hour, 4 hours, and 24 hours. The observations were recorded in a table with the description “clear” if there was no precipitate formed in the solution, “opaque” if the solution was clear with some cloudiness, and “precipitate” if a precipitate or particles had formed. Examples of the different observation types are shown in Figure 8.

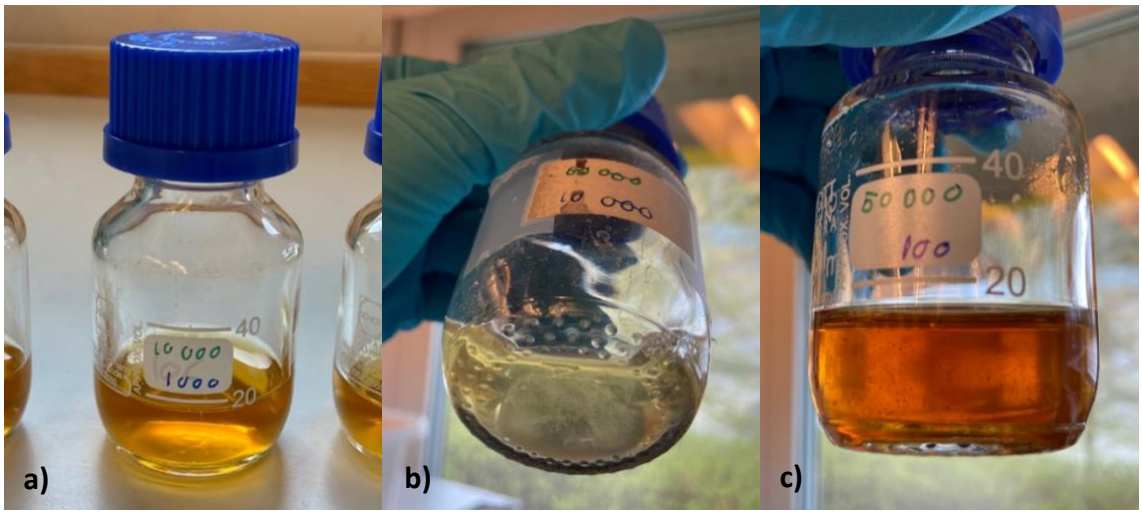

Figure 8: Example images of the three observation types a) Clear b) Opaque c) Precipitate from calcium compatibility testing.

3. Project A: Aminosuccinate methylenephosphonated scale inhibitors

Phosphonate functional groups are known to improve scale inhibition, which is why the goal of project A was to synthesize aminomethylenephosphonate scale inhibitors. The different projects involved phosphonation of one, two and three methylenephosphonate groups, to investigate the efficiency of the different SIs along with potential biodegradability. Further, high biodegradation was optimal where the minimum requirement set by OSPAR was a biodegradability > 20%.

3.1. Project 1: Phosphonated tetrasodiumiminodisuccinate

3.1.1. Chemicals

Tetrasodiumiminodisuccinate (TSIDS) is a sodium salt of iminodisuccinic acid. It is sold by Bayer (Lanxess) as a solution water as a biodegradable chelate, scale dissolver, or builder in detergents. This project involved phosphonating TSIDS by addition of one methylene phosphonate group with the goal of achieving high biodegradation and effective scale inhibition. Phosphonated TSIDS (TSIDS-P) was tested against $BaSO_4$ and $CaCO_3$ scale on the high-pressure dynamic tube blocking rig. The results were measured against commercial scale inhibitors (Mady et al., 2021).

3.1.2. Synthesis

TSIDS-P was synthesized using the Moedritzi-Irani reaction following the procedure in 2.3. One methylene phosphonate group was attached to the secondary amine in the centre of TSIDS as shown in Figure 9. ^{31}P NMR with coupling showed one triplet peak at 6.33 clearly indicating phosphonation of one product. However, The NMR was not conclusive enough to give an exact product.

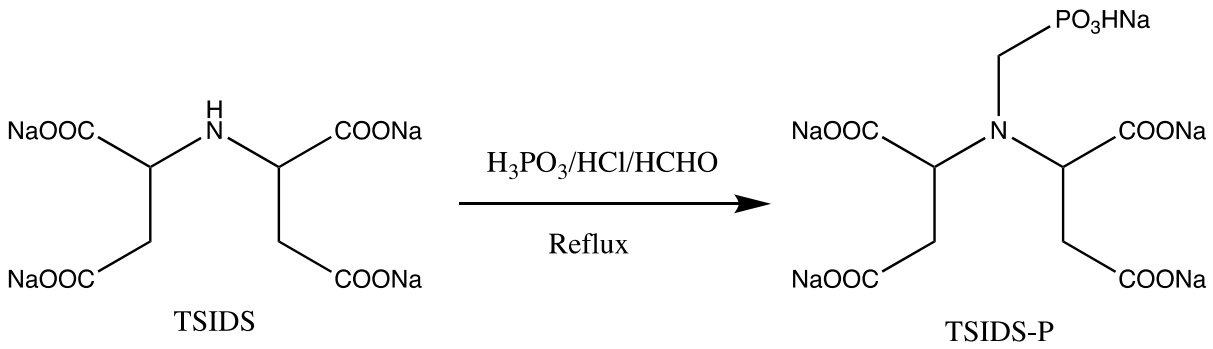

Figure 9: Methylene phosphonate derivative synthesis of TSIDS via Moedritzi-Irani.

Various parameters used for the synthesis attempts of TSIDS-P are shown in Table 6. Several attempts were made to yield optimal scale inhibition for TSIDS-P. All attempts were tested on the high-pressure dynamic tube blocking rig against calcite scaling, except the test (0) attempt.

Table 6: Parameters for each synthesis attempt using Moedritzi-Irani on TSIDS.

Attempt number	TSIDS (g)	H_3PO_3 (mol equivalents)	HCl (mol equivalents)	HCHO (mol equivalents)	Temperature (°C)	Reflux time (hours)
0 (Test)	2.00	1	1	1	110	48
1	2.00	2.5	6	3	110	24
2	2.00	1.2	6	1.5	110	24
3	2.00	1.2	6	1.5	110	24
4	2.00	1.2	6	1.5	110	48
5	2.00	1.2	6	1.5	115	24
6	2.00	1.2	6	1.5	115	24
7	2.00	1.2	6	1.5	115	24

3.1.3. Results and discussion

3.1.3.1. Synthesis attempts

In the test attempt (0), the mol equivalents were not sufficient to synthesize TSIDS-P. Therefore, mol equivalents had to be increased to make the synthesis work. For the first attempt mol equivalents were increased and the reflux time was set to 24 hours, which resulted in a successful synthesis of TSIDS-P. However, when the solution was made into a SI solution (Appendix A, 0), the FIC was at 50 ppm, possibly indicating some impurities in the solution. Therefore, for the second attempt, mol equivalents of H_3PO_3 and HCHO were reduced. The solution was neutralized and tested on the rig where the result was 50 ppm with observations of calcium incompatibility from 100-50 ppm. Therefore, the solution was tested a second time starting from 50 ppm instead of 100 ppm. This attempt had an FIC at 5 ppm. The same attempt was also crystalized to remove the liquid of solution and leave the solid material for testing. A few crystals were made into a SI solution and tested on the rig, yielding an FIC of 50 ppm. The same amount of mol equivalents were used for the remaining attempts. On the third attempt the solution was neutralized and ran on the rig without any further alterations, this yielded an FIC of 10 ppm. For the fourth attempt, the same was done as in attempt three, only with an increased reflux time (48 hrs). The result was an FIC of 20 ppm. In the fifth attempt, the solution was filtered to remove particles and leave only the aqueous solution. This attempt resulted in an FIC of 50 ppm. Attempt number six was tested by neutralization of the whole solution. The first scale test gave an FIC of 50 ppm, but the second scale gave an FIC of 10 ppm. This inconsistency in FIC values likely occurred due to air bubbles in the injection line of the rig. This would slow down the injection rate, resulting in large discrepancies in FIC values between the first and second scale test. Finally, for attempt seven, the whole solution was neutralized before being tested. This resulted in a consistent FIC of 10 ppm as shown in Figure 10.

3.1.3.2. Scaling tests

TSIDS-P was tested against calcite and barite scaling on the high-pressure dynamic tube blocking rig. The results are presented in Figure 10 and Figure 11. TSIDS-P gave an FIC of 10 ppm and 3 minutes after the first scale test, and an FIC of 10 ppm and 15 minutes after the second scale when tested against calcite scaling. These are consistent results that indicate that the MIC for TSIDS-P will be between 20 ppm and 10 ppm. A list of commercial SIs tested on the same rig as our tests can be viewed in Table 7. The scaling results of TSIDS-P against calcite scaling are improved compared to ATMP, another phosphonated SI. However, our SI

did not exceed the FIC values of both phosphonoacetic acid (PAA) and PVS. Therefore, we can conclude that TSIDS-P showed moderate scale inhibition against calcite scale. Indication of calcium incompatibility can be seen in Figure 10 from 100 ppm to 20 ppm in the first scale test. This was investigated with a calcium compatibility test.

The result from TSIDS-P against barite scaling gave an FIC at 100 ppm and 20 minutes after the first scale, and the second scale occurred at an FIC at 100 ppm and 13 minutes. Evidently, TSIDS-P gave poor results against barite scaling. This is especially apparent when compared to the barite inhibition of DTPMP and PVS.

Table 7: FIC concentration of commercial scale inhibitors tested against calcite and barite scaling.

SI	Scale type	1st scale		2nd scale	
		Concentration (ppm)	Time (min)	Concentration (ppm)	Time (min)
Phosphonoacetic acid	Calcite	5	14	5	12
ATMP	Calcite	20	44	20	46
PVS	Calcite	2	8	2	10
PVS	Barite	5	5	5	4
DTPMP	Barite	10	13	10	12

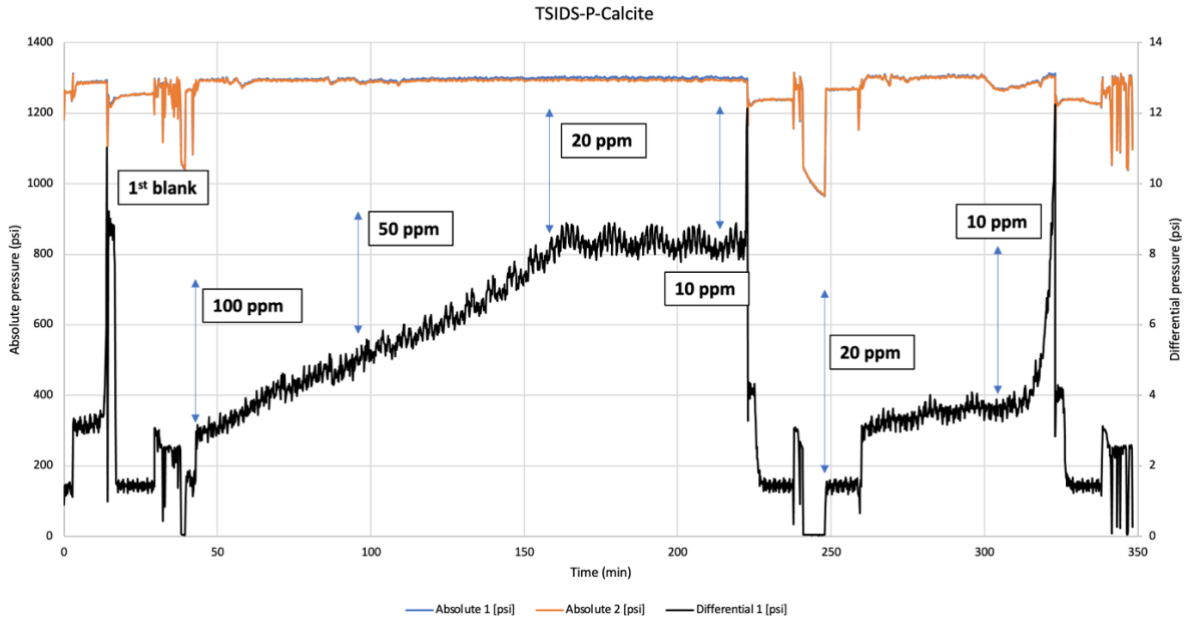

Figure 10: Differential pressure and time results from high-pressure dynamic tube blocking experiments of TSIDS-P against calcite scaling.

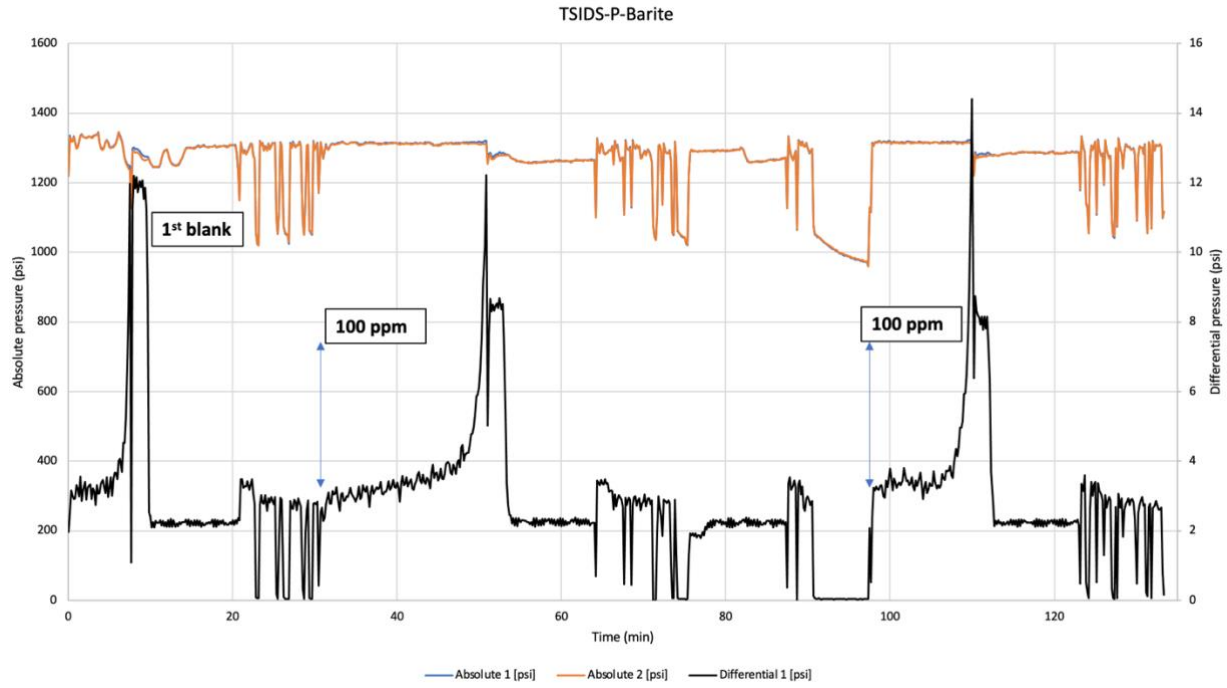

Figure 11: Differential pressure and time results from high-pressure dynamic tube blocking experiments of TSIDS-P against barite scaling.

3.1.3.3. Calcium compatibility testing

Table 8 show calcium compatibility testing of TSIDS-P with different concentrations of SI (100, 1000, 10000, 50000) mixed with different concentrations of Ca^{2+} solution (100, 1000, 10000). The results indicate that all SI concentrations at 50 000 ppm formed a precipitate with all dosages of Ca^{2+} (100, 1000, 10000) after 4 hours and 24 hours. This is a difficult test as the concentration of SI is high and will likely complex bind to Ca^{2+}. This concludes that the possible calcium incompatibility shown in the scaling test (Figure 10) was indeed correct as TSIDS-P was not compatible at high concentrations of SI and Ca^{2+}. Therefore, squeeze treatment would not work for TSIDS-P as precipitation due to Ca^{2+}-SI complex can cause formation damage. However, TSIDS-P could work topside by continuous injection where there are lower Ca^{2+} concentrations.

Table 8: Calcium compatibility test of TSIDS-P with mixtures of Ca^{2+} concentrations (100, 1000, 10000) and SI concentrations (100, 1000, 10000, 50000).

SI	Ca^{2+} dose (ppm)	SI dose (ppm)	Appearance				
			After mixing	30 min	1 hour	4 hours	24 hours
TSIDS-P	100	100	Clear	Clear	Clear	Clear	Clear
		1000	Clear	Clear	Clear	Clear	Clear
		10000	Clear	Clear	Clear	Clear	Clear
		50000	Clear	Clear	Clear	Precipitate	Precipitate
	1000	100	Clear	Clear	Clear	Clear	Clear
		1000	Clear	Clear	Clear	Clear	Clear
		10000	Clear	Clear	Clear	Clear	Clear
		50000	Clear	Clear	Clear	Precipitate	Precipitate
	10000	100	Clear	Clear	Clear	Clear	Clear
		1000	Clear	Clear	Clear	Clear	Clear
		10000	Clear	Clear	Clear	Clear	Clear
		50000	Clear	Clear	Clear	Precipitate	Precipitate

3.1.3.4. Biodegradability

Biodegradability tests of TSIDS and TSIDS-P are presented in Table 9 with a sodium benzoate solution as a control test using the OECD 306 method. From the bottles tested, one bottle gave 34.5% biodegradation for TSIDS. This was the most reliable result as TSIDS is a water-based biodegradable chelate, and it matched the results from TSIDS-P. TSIDS-P showed exceptional biodegradability with an average of 72.56% across all bottles tested. OSPAR regulations requires minimum > 20% biodegradation for usage and discharge in the North Sea. As biodegradability is the biggest factor for satisfying these regulations, > 20% biodegradability is highly valued. Biodegradability > 60% is considered exceptional, which makes TSIDS-P readily biodegradable.

Table 9: Biodegradability testing of TSIDS and TSIDS-P using the OECD 306 method over 28 days.

Compound/SI	**Biodegradability by OECD 306 (%)**
Sodium benzoate	80.14
TSIDS	34.5
TSIDS-P	72.56

3.1.4. Further study

Further studies for this project could include thermal stability testing to check how TSIDS-P would fair in high temperature conditions. Thermal ageing is a technique that could be used to check this. A new test on the high-pressure dynamic tube blocking rig after thermal ageing would show if high temperatures impacted the calcite inhibition. Also, crystallization could be an option to achieve a purer product of TSIDS-P. This could possibly result in more conclusive NMR, which could lead to greater scale inhibition.

3.2. Project 2: Phosphonated tetrasodium ethylenediaminodisuccinate

3.2.1. Chemicals

Tetrasodium ethylenediaminodisuccinate (TSEDAS) is a sodium salt containing two amine groups. The goal of this project was to add two methylene phosphonate groups to TSEDAS using the Moedritzi-Irani reaction to yield biodegradability > 20% and efficient scale inhibition. Bisphosphonated TSEDAS (TSEDAS-P) was tested against $BaSO_4$ and $CaCO_3$ scale on the high-pressure dynamic tube blocking rig. The results were measured against commercial scale inhibitors.

3.2.2. Synthesis

By following the procedure described in 2.3, the Moedritzi-Irani reaction was performed to complete a bisphosphonation of TSEDAS where methylene phosphonates were attached to the two secondary amines as shown in Figure 12. ^{31}P NMR with coupling showed two triplet peaks at 8.93 and 8.32 (Appendix C, Figure 35). These results suggested phosphonation of two products were there should only be one triplet peak (one product).

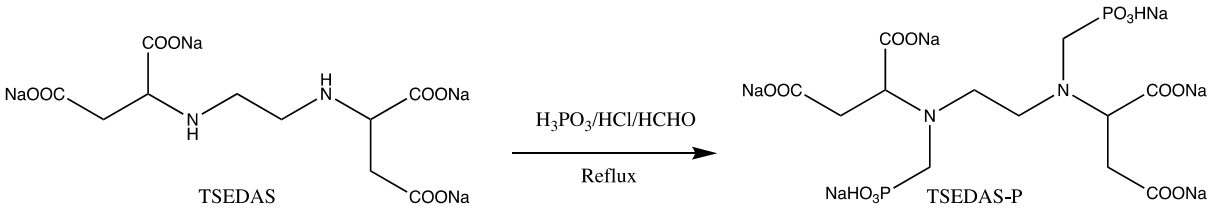

Figure 12: Methylene phosphonate synthesis of TSEDAS via Moedritizi-Irani.

Different parameters used for the synthesis attempts of TSEDAS-P are displayed in Table 10. Here, different parameters were adjusted until optimal results were achieved in attempt three. All synthesis attempts were tested on the high-pressure dynamic tube blocking rig against calcite scaling.

Table 10: Parameters for each synthesis attempt of TSEDAS via Moedritzi-Irani.

Attempt number	TSEDAS (g)	H_3PO_3 (equivalents)	HCl (equivalents)	HCHO (equivalents)	Temperature (°C)	Reflux time (hours)
1	1.5	3	7	4	110	24
2	1.0	2.4	7	3	110	24
3	1.0	3	7	3	115	24

3.2.3. Results and discussion

3.2.3.1. Synthesis attempts

The first attempt included the mol equivalents seen in Table 10 where seven mol equivalents of HCl was needed. Here, four mol equivalents were needed for the sodium carboxylate groups, in addition, one mol equivalent HCl per secondary amine group. Additionally, an extra mol

equivalent HCl was added to make certain that the reaction would work. It was evident that there were excess HCHO from the reaction, which is why both the amounts of H_3PO_3 and HCHO were reduced. The second attempt had reduced mol equivalents, which resulted in great scale inhibition on calcite scale. However, NMR did not show a clear phosphonation, therefore, the mol equivalents of H_3PO_3 were increased to three for the third attempt. The third attempt gave clear NMR results of phosphonation (Appendix C, Figure 35) and gave great results on calcite scale on the rig.

3.2.3.2. Scaling tests

Figure 13 and Figure 14 show the results from the high-pressure dynamic tube blocking rig after testing of TSEDAS-P against calcite scaling. Due to air bubbles blocking the injection lines during testing, a repeat test of TSEDAS-P was necessary to give consistent results. The repeat test acted as the "second scale test" as difficulties with the rig did not allow for a full test (blank-chemical-repeat chemical) to be performed. The first scale test had an FIC at 5 ppm and 23 minutes, and the second scale test had an FIC at 5 ppm and 28 minutes. This would indicate an MIC between 10 ppm and 5 ppm. By comparing our results to commercial SIs (Table 7), TSEDAS-P showed improved calcite scale inhibition compared to ATMP, and similar inhibition to PAA. PVS showed superior results, but we can still conclude that TSEDAS-P displayed excellent inhibition against calcite scaling. The indicated MIC for our SI would be between 10 ppm and 5 ppm. No indication of calcium incompatibility was observed (Figure 13 and Figure 14). However, a calcium compatibility test was run for validation.

Figure 15 and Figure 16 show the results from testing of TSEDAS-P against barite scale on the high-pressure dynamic tube blocking rig. The rig faced the same problems as with the calcite scaling tests, therefore, a repeat test was performed for barite scaling as well. The first scale had an FIC at 100 ppm and 9 minutes, and the second scale had an FIC at 100 ppm and 31 minutes. Compared to DTPMP and PVS, TSEDAS-P gave poor barite inhibition.

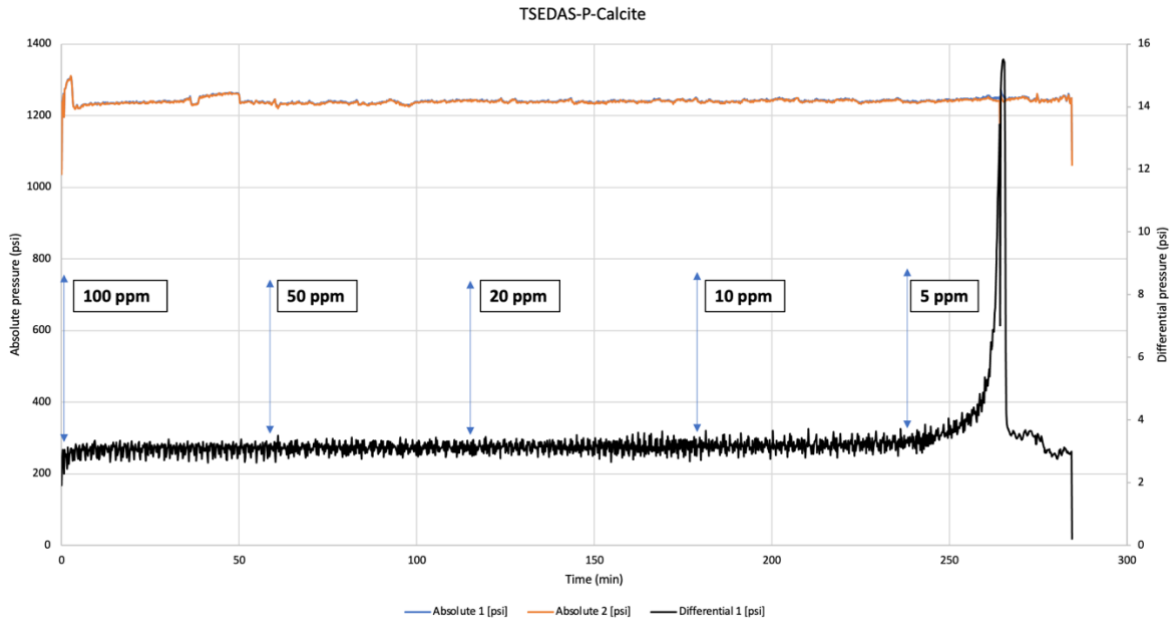

Figure 13: Differential pressure and time results from high-pressure dynamic tube blocking experiments of TSEDAS-P against calcite scaling.

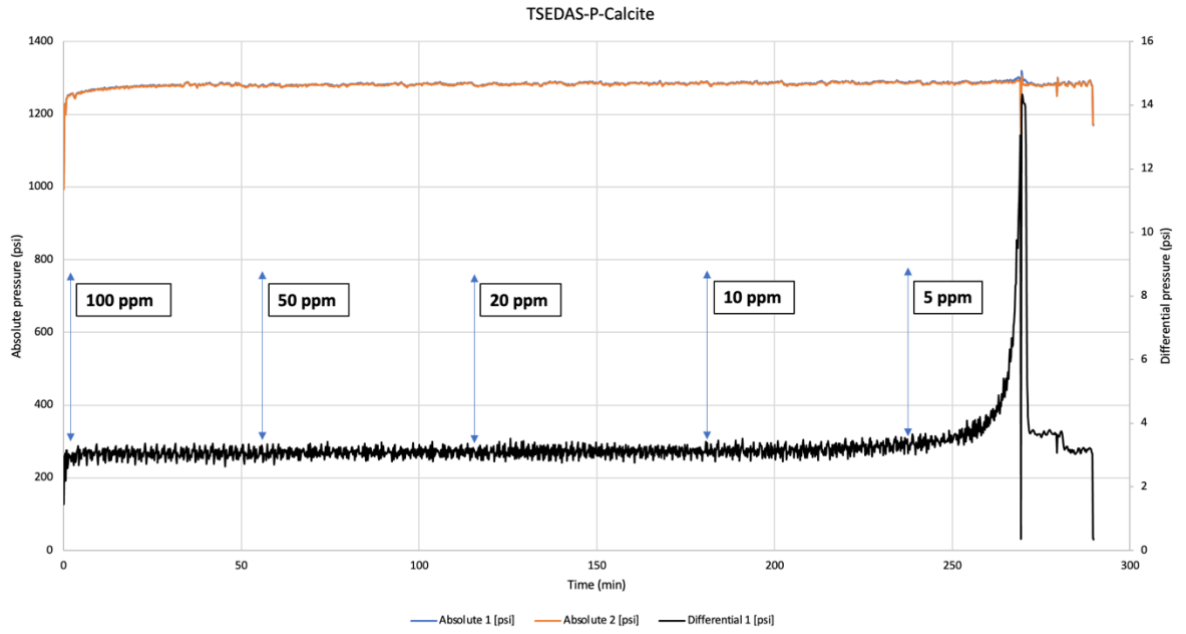

Figure 14: Differential pressure and time results from high-pressure dynamic tube blocking experiments of TSEDAS-P repeat test against calcite scaling.

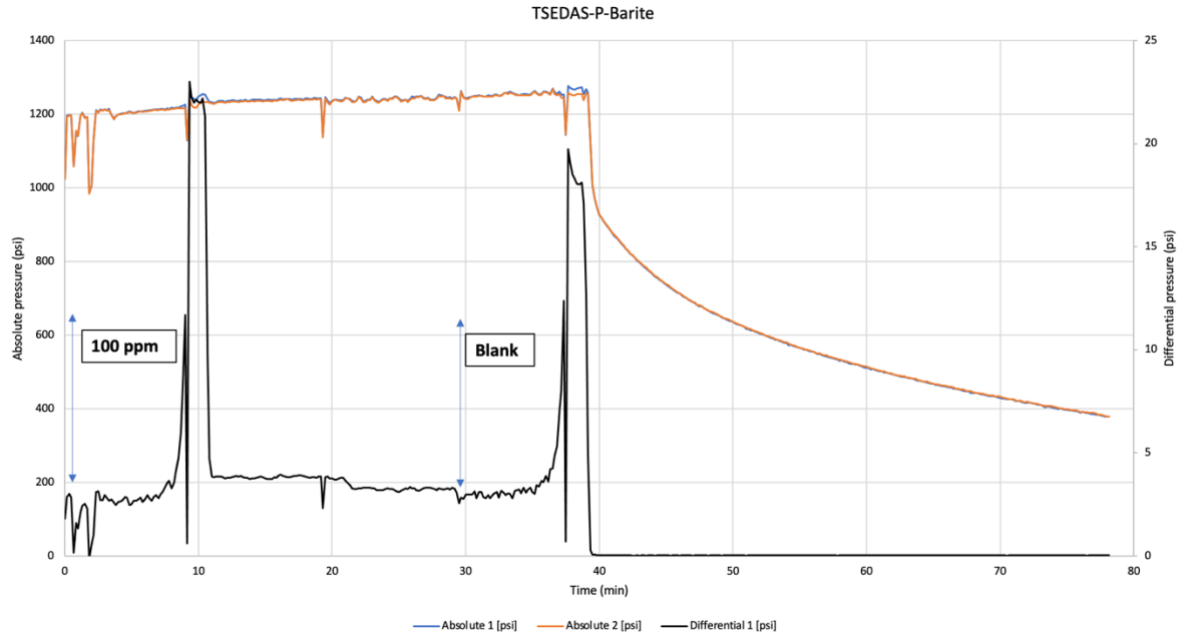

Figure 15: Differential pressure and time results from high-pressure dynamic tube blocking experiments of TSEDAS-P against barite scaling.

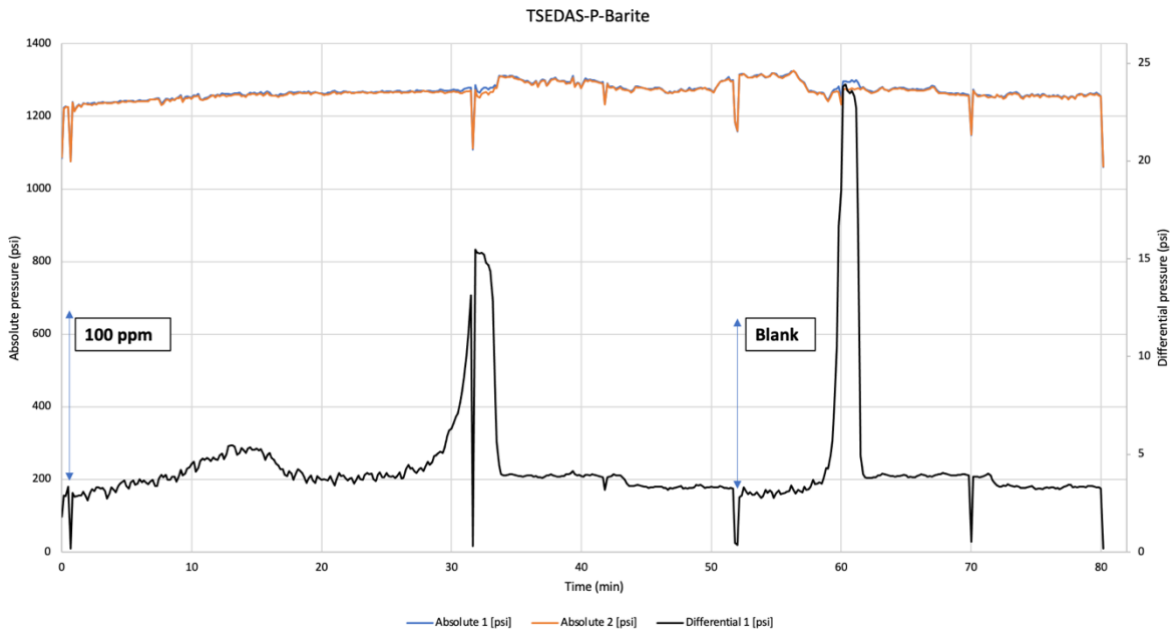

Figure 16: Differential pressure and time results from high-pressure dynamic tube blocking experiments of TSEDAS-P repeat test against barite scaling.

3.2.3.3. Calcium compatibility testing

The results for calcium compatibility testing of TSEDAS-P are presented in Table 11. Here, the results showed clear solutions at all concentration mixtures except at 50000 ppm SI and 1000 ppm Ca^{2+} after 4 and 24 hours. These were observed as opaque, which does not indicate a precipitate. Also, opaque/cloudiness is not expected to be detrimental to the flow during injection. Therefore, TSEDAS-P could be used for squeeze treatment injection where formations have high concentrations of Ca^{2+}.

Table 11: Calcium compatibility test of TSEDAS-P with mixtures of Ca^{2+} concentrations (100, 1000, 10000) and SI concentrations (100, 1000, 10000, 50000).

SI	Ca^{2+} dose (ppm)	SI dose (ppm)	Appearance				
			After mixing	30 min	1 hour	4 hours	24 hours
TSEDAS-P	100	100	Clear	Clear	Clear	Clear	Clear
		1000	Clear	Clear	Clear	Clear	Clear
		10000	Clear	Clear	Clear	Clear	Clear
		50000	Clear	Clear	Clear	Clear	Clear
	1000	100	Clear	Clear	Clear	Clear	Clear
		1000	Clear	Clear	Clear	Clear	Clear
		10000	Clear	Clear	Clear	Clear	Clear
		50000	Clear	Clear	Clear	Clear	Clear
	10000	100	Clear	Clear	Clear	Clear	Clear
		1000	Clear	Clear	Clear	Clear	Clear
		10000	Clear	Clear	Clear	Clear	Clear
		50000	Clear	Clear	Clear	Opaque	Opaque

3.2.3.4. Biodegradability

Biodegradability was tested using the OECD 306 method for TSEDAS and TSEDAS-P with a sodium benzoate solution as a control test. The results are shown in Table 12. The expected percent biodegradability of sodium benzoate should be about 80%. Therefore, the control solution was indeed valid. TSEDAS and TSEDAS-P both displayed poor biodegradability. The minimum required rate of biodegradation for green oilfield chemicals is > 20%. This requirement was not met by either the base chemical or the bisphosphonated one, therefore, these would not be considered readily biodegradable. This could indicate that multiple methylene phosphonate functional groups may result in decreased biodegradability for TSEDAS.

Table 12: Biodegradability testing of TSEDAS and TSEDAS-P using the OECD 306 method over 28 days.

Compound/SI	Biodegradability by OECD 306 (%)
Sodium benzoate	80.14
TSEDAS	0
TSEDAS-P	2.68

3.2.4. Further study

Since TSEDAS-P showed excellent calcium compatibility and great scale inhibition against calcite scaling, a thermal stability test could be beneficial. Thermal stability testing could be performed to check how TSEDAS-P would tolerate high temperatures and if it would affect the scaling inhibition. This could be checked by a repeat test on the high-pressure dynamic tube blocking rig after a thermal stability test. A thermal stability test would also indicate if TSEDAS-P could be used in squeeze treatment applications. Additionally, TSEDAS-P could be crystallized to achieve a purer product yielding conclusive NMR and possibly perform better on the rig. Lastly, TSEDAS could be synthesized with only one methylene phosphonate group to see if this would yield any improved scale inhibition compared to the current bisphosphonated TSEDAS. Addition of only one methylene phosphonate group could possibly improve biodegradability.

3.3. Project 3: Phosphonated ethylenediamine- and diethylenetriamine Bis-*N,N'*-Succinic acid

3.3.1. Chemicals

The goal of this project was to synthesize a polyamide with three methylene phosphonate groups to see if it would yield effective scale inhibition. To achieve this, a two-step synthesis was required. Firstly, a chelate would be synthesized where attempts of synthesis were made using ethylenediamine (EDA) and diethylenetriamine (DETA). Secondly, a Moedritzi-Irani synthesis where the newly made chelate was phosphonated.

3.3.2. Synthesis

Maleic anhydride was reacted with EDA and DETA in the two synthesis attempts. The procedure for the synthesis of EDA bis-*N,N*-succinic acid (EDAS) and DETA bis-*N,N*-succinic acid (DETAS) was based on a patent by Kezerian & Ramsey (n.d.).

Maleic anhydride (10g) was dissolved in deionized water (10 mL) and stirred with a magnetic stirrer in a round bottom Erlenmeyer flask with a second funnel for one hour. Afterwards, the solution was set in an oil bath at 75°C and connected to a condenser with a water inlet and outlet, creating a reflux. A 50% NaOH solution was prepared by addition of solid NaOH (8.5g) to a glass beaker and dissolved with deionized water (8.5g). The 50% NaOH solution (total 17.0g) was added dropwise using a titrator attached to the second funnel of the Erlenmeyer flask along with 5 mL of deionized water. After titration of NaOH, the titrator was washed and the temperature was increased to 80°C before EDA (0.1 mol =6.147g) was added dropwise using the same titrator. Finally, 15 mL deionized water was added before the temperature was increased to 115°C and the solution was left to reflux for 24 hours. The synthesis for the reaction is shown in Figure 17. Next, the solution was adjusted to pH 2 by dropwise addition of HCl (37 wt%). Thereafter, the Moedritzi-Irani reaction could be applied to phosphonate the compound.

However, synthesis of EDAS was not easily characterized with mass spectrometry. The addition of a single succinic acid to only one of the three available substitution sites on the primary or secondary amine was challenging to achieve. Due to the tedious nature of the procedure and insecurities of characterization of EDAS, we decided to proceed with DETAS. Synthesis of EDAS was not pursued further for this project.

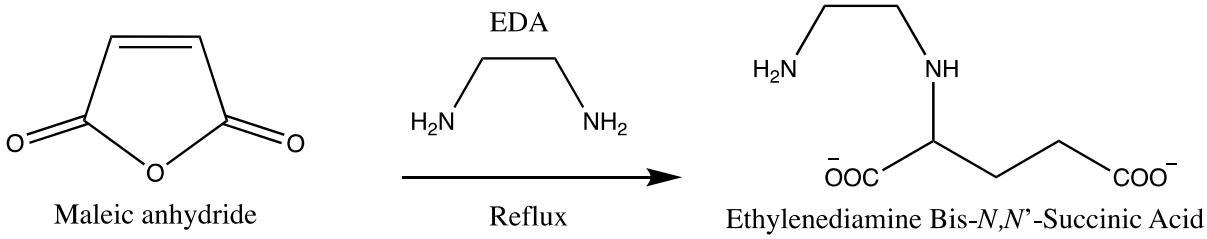

Figure 17: Synthesis of EDAS by reaction of maleic anhydride with EDA.

Synthesis of DETAS was achieved following the same procedure as described for EDAS. However, after titration of NaOH, the temperature was increased to 80°C and DETA (0.05 mol = 5.16g) was added dropwise using the same titrator. After titration, 15 mL deionized water was added, and the temperature was increased to 115°C and left to reflux for 48 hours. The synthesis for the reaction can be seen in Figure 18. Next, the solution was adjusted to pH 3.3 by dropwise addition of concentrated HCl (37 wt%). Thereafter, the Moedritzi-Irani reaction was used to methylene phosphonate our product where three methylene phosphonates were attached to the secondary amines. Equivalents used for the Moedritzi-Irani reaction were 3.6 mol equivalents H_3PO_3, 10 mol equivalents HCl, and 4.5 mol equivalents HCHO. The Moedritzi-Irani procedure was followed as previously described in 2.3.

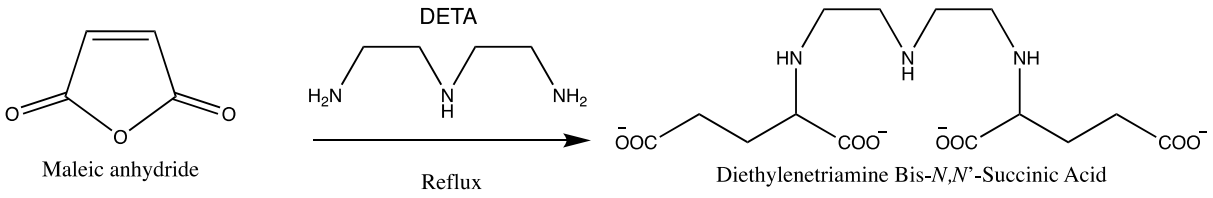

Figure 18: Synthesis of DETAS by reaction of maleic anhydride with DETA.

3.3.3. Results and discussion

3.3.3.1. Scaling tests

DETAS-P was tested against calcite scaling on the high-pressure dynamic tube blocking rig. The results are presented in Figure 19. The first scale had an FIC of 50 ppm and 40 minutes, and the second scale occurred at 50 ppm and 56 minutes. This would indicate that the MIC would be between 100 ppm and 50 ppm. It was observed that the SI solution was only partially soluble, which could explain the poor inhibition results. Because the solution was not completely soluble the project was not pursued further.

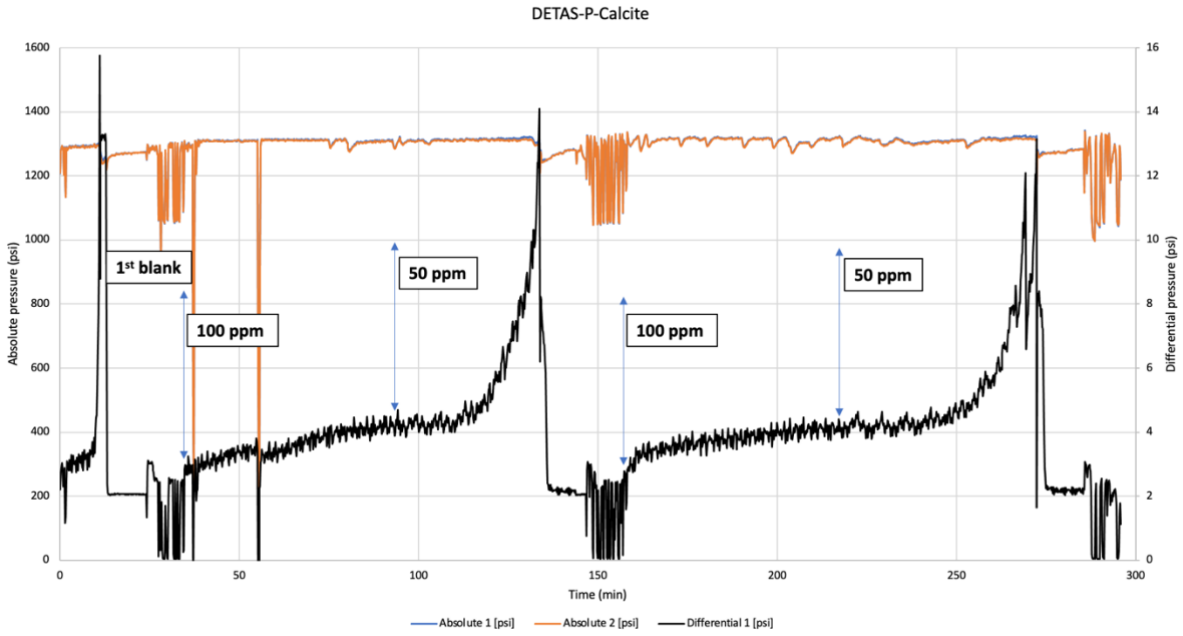

Figure 19: Differential pressure and time results from high-pressure dynamic tube blocking experiments of phosphonated diethylenetriamine bis-N,N'-Succinic Acid against calcite scaling.

4. Project B: Phosphonated glucosamine as scale inhibitor

4.1. Chemicals

Glucosamine is a monomer of the natural chitosan polysaccharide (Figure 20), which comes from crustacean shells. This project was based on a paper by Mady *et al.* (2021) where chitosan was phosphonated. Phosphonated chitosan (PCH) gave moderate calcite inhibition and poor barite inhibition. The molecular dynamics study showed that PCH was randomly folded where the interaction sites were minimized to attach to the mineral surfaces (Mady et al., 2021). Therefore, the goal of this project was to phosphonate one part (glucosamine) of the chitosan polymer to yield efficient scale inhibition. The phosphonated glucosamine (glucosamine-P) was tested against $CaCO_3$ and $BaSO_4$ scale on the high-pressure dynamic tube blocking rig. The results were measured against commercial SIs.

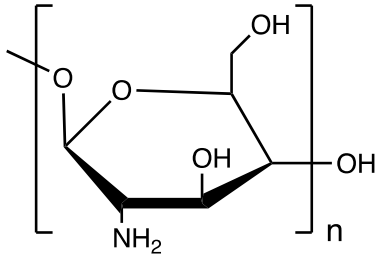

Chitosan

Figure 20: Chemical structure of chitosan polysaccharide.

4.2. Synthesis

Glucosamine was first synthesized via conventional Moedritzi-Irani reaction by reflux. The synthesis can be seen in Figure 21. Here, two methylene phosphonate groups were attached to the primary amine of glucosamine. ^{31}P NMR with coupling suggested phosphonation (Appendix D, Figure 39). However, the carbohydrate ring could be opened even before the phosphonate group is attached. This would result in the structure shown in Figure 22. The ball milling method was also used to synthesize glucosamine-P. Here, ^{31}P NMR with coupling implied phosphonation (Appendix D, Figure 47). This method would also synthesize glucosamine-P via Moedritzi-Irani but is considered a costlier method. The synthesis attempts of glucosamine-P via reflux are shown in Table 13 and synthesis attempts via ball milling are displayed in Table 14.

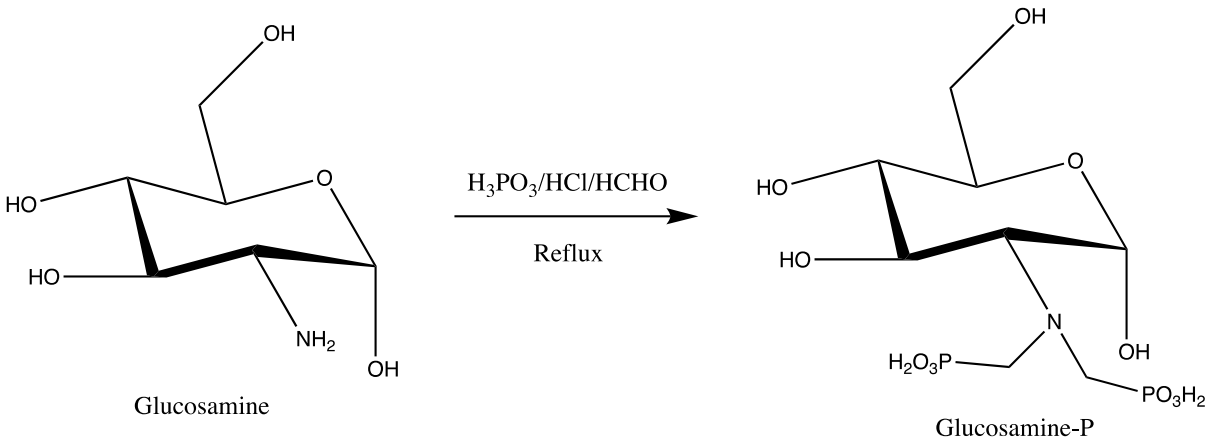

Figure 21: Synthesis of methylene phosphonate of glucosamine via Moedritzi-Irani method.

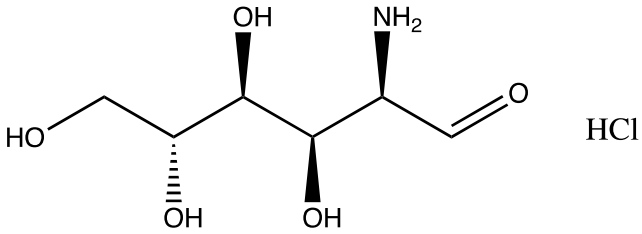

Figure 22: Ring-opened glucosamine hydrochloride after Moedritzi-Irani.

Parameters used for the synthesis attempts of glucosamine-P via reflux are presented in Table 13. Evidently, reflux times were reduced to find the optimal time window for the reaction.

Table 13: Parameters used for Moedritizi-Irani synthesis on glucosamine via reflux.

Attempts	Glucosamine (g)	H_3PO_3 (mol equivalents)	HCl (mol equivalents)	HCHO (mol equivalents)	Reflux time (hours)
1	1.60	2	2	2	48
2	1.00	2	2	2	4
3	1.00	2	2	2	8
4	1.00	2	2	2	2

The different parameters used for the synthesis attempts of glucosamine-P via ball milling are displayed in Table 14. The first attempt was synthesized in one of the zirconium bowls (the second bowl was empty but placed in for stabilization) with the parameters shown. Attempts two and three were synthesized together in the two available zirconium bowls. Attempt two did not contain any distilled water but attempt three contained 0.5 mL of distilled water. For this reaction, the RPM was increased to 700 and the repetitions were increased to 24.

Table 14: Parameters used for Moedritzi-Irani synthesis of glucosamine via ball milling method.

Attempts	Glucosamine (g)	H_3PO_3 (mol equivalents)	P(HCHO) (mol equivalents)	Distilled water (mL)	RPM	Milling (min)	Reps
1	1.00	2	2	N/A	600	20	12
2	1.00	2	2	N/A	750	20	24
3	1.00	2	2	0.5	750	20	24

4.3. Results and discussion

4.3.1. Synthesis attempts

Table 13 shows several attempts made to synthesize glucosamine using the Moedritzi-Irani reaction. The first attempt had a long reflux time of 48 hours where the NMR results were inconclusive. Therefore, the reflux time was significantly reduced in the second attempt. Here, NMR was more conclusive (Appendix D, Figure 39) and the product was neutralized. The product was a yellow/orange colour. This attempt was tested on the high-pressure dynamic tube blocking rig against calcite scaling resulting in an FIC of 20 ppm and 35 minutes. The reflux time was increased for the third attempt to see if this would give greater scale inhibition. However, the result was a degraded dark brown/black coloured product that gave an FIC at 50 ppm and 54 minutes for calcite scaling. The fourth and final attempt had a reaction time of two hours and resulted in a light-yellow colour. This attempt was tested against calcite scaling resulting in an FIC at 100 ppm and 41 minutes possibly indicating an incomplete phosphonation reaction because of too low reflux time.

Evidently, the product seemed to degrade after longer reflux times, which is why the reflux times were reduced. A reflux time of four hours gave the most promising result. However, the ring structure could be opened due to high temperatures during reflux. Therefore, we decided that a good option would be to try the ball milling method as the temperature would reach a maximum of 90°C. This could possibly keep the ring structure closed.

The attempts for synthesis of glucosamine using the ball milling method are displayed in Table 14. The first attempt resulted in an orange/brown product (Figure 23). The product was tested against calcite scaling, resulting in an FIC at 20 ppm and 11 minutes. The results for attempt two and three using ball milling are shown in Figure 24. Here, Figure 24 a) shows a dark black/dark brown degraded product of glucosamine-P-Ballmill-No H2O, and b) displays a yellow/orange coloured product of glucosamine-P-Ballmill-With H2O, seemingly not degraded.

Figure 23: First attempt of Moedritzi-Irani synthesis of glucosamine using ball milling method.

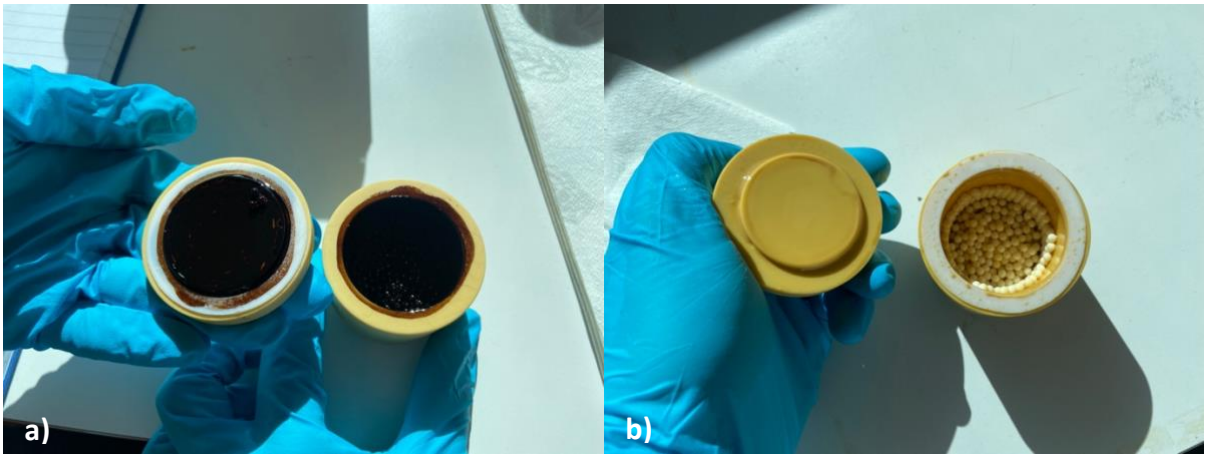

Figure 24: Moedritzi-Irani synthesis using ball milling method. a) Glucosamine-P-Ballmill-No H_2O b) Glucosamine-P-Ballmill-With H_2O.

Glucosamine-P-ballmill-No H_2O was characterized using ^{31}P NMR where the results suggested multiple products (Appendix D, Figure 51) and could possibly indicate ring-opening. As previously mentioned, the product had a degraded colour, and due to the inconsistent NMR results, this would not be easily replicated. A possible explanation for the degraded colour and ring-opening could be due to the aggressive reaction without the presence of water. On the other hand, glucosamine-P-ballmill-With H_2O showed one peak in ^{31}P NMR suggesting a single product (Appendix D, Figure 47). Here, the reaction seems to have yielded the phosphonated product we wanted and therefore, this could be replicated for further testing. The colour of the product also looked purer.

4.3.2. Scaling tests

Glucosamine-P-ballmill-With H_2O was tested against calcite scaling on the high-pressure dynamic tube blocking rig. The results are presented in Figure 25. The first scale resulted in

an FIC at 10 ppm and 25 minutes, and the second scale gave an FIC at 10 ppm and 47 indicating an MIC between 20 ppm and 10 ppm. Compared to the commercial SIs in Table 7, the scale inhibition of our SI against calcite scaling was improved compared to ATMP, similar to PAA, yet not better than PVS. Resulting in glucosamine-P-ballmill-With H_2O to yield moderate calcite scale inhibition.

Glucosamine-P-With H_2O was also tested against barite scaling on the high-pressure dynamic tube blocking rig (Figure 26). The result of the first scale was an FIC at 100 ppm and 49 minutes, and the second scale had an FIC at 100 ppm and 29 minutes. Our SI showed poor scale inhibition against barite scaling, especially when compared to PVS and DTPMP in Table 7.

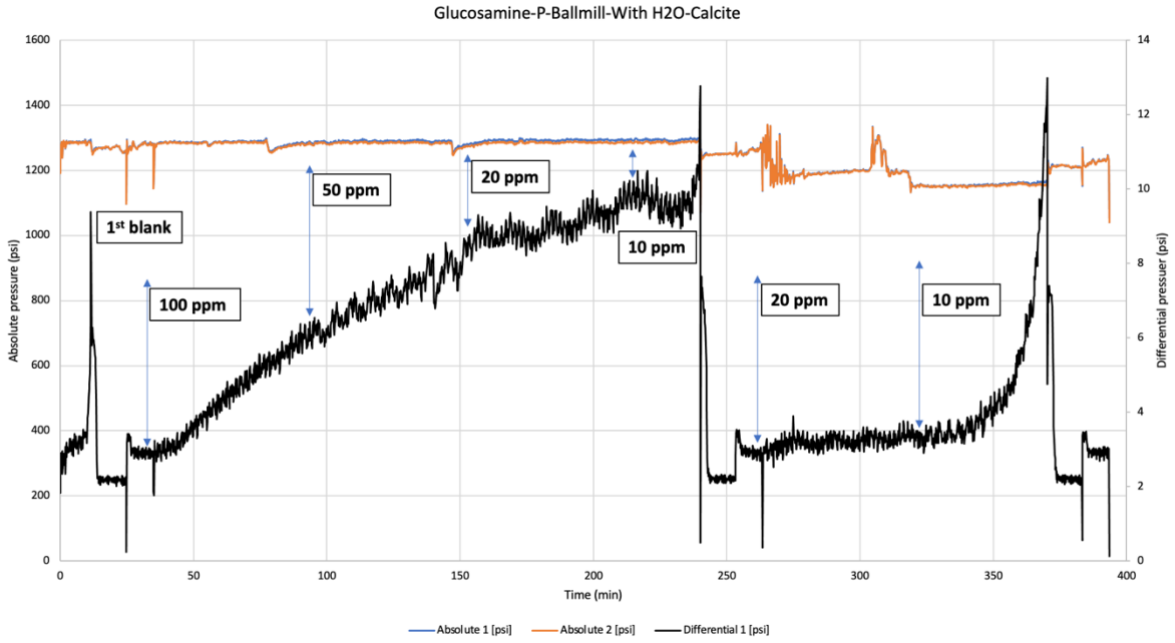

Figure 25: Differential pressure and time results from high-pressure dynamic tube blocking experiments of glucosamine-P-ballmill-With H_2O against calcite scaling.

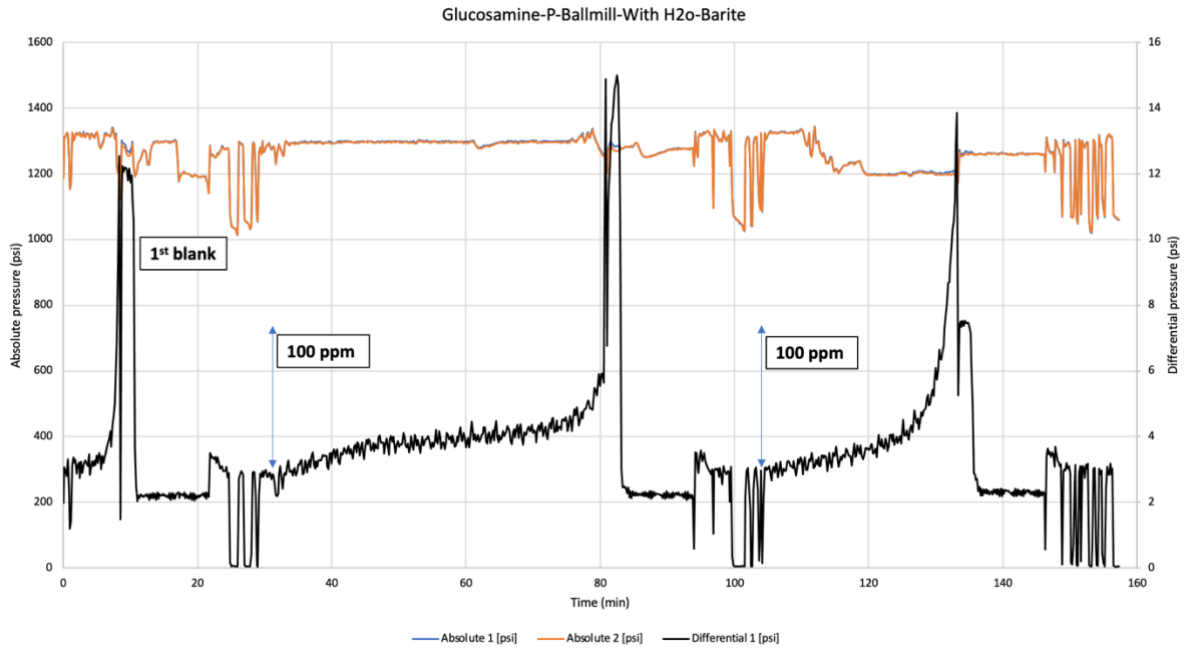

Figure 26: Differential pressure and time results from high-pressure dynamic tube blocking experiments of glucosamine-P-With H_2O against barite scaling.

Glucosamine-P-No H_2O was tested against calcite scale on the high-pressure dynamic tube blocking rig. Here, the first scale gave an FIC at 5 ppm and 7 minutes, and the second scale resulted in an FIC at 5 ppm and 17 minutes. This would indicate an MIC value between 10 ppm and 5 ppm. The results show great calcite scale inhibition even when compared to the commercial SIs in Table 7. Our SI showed improved calcite inhibition results compared to ATMP and similar results to PAA. However, our SI did not give FIC values better than that of PVS.

Glucosamine-P was also tested against barite scaling on the same rig. Here, the first scale resulted in an FIC at 20 ppm and 3 minutes, and the second scale gave an FIC at 20 ppm and 9 minutes. These results imply an MIC between 50 ppm and 20 ppm which could be considered as decent barite inhibition. However, our results were not improved compared to DTPMP and PVS (Table 7).

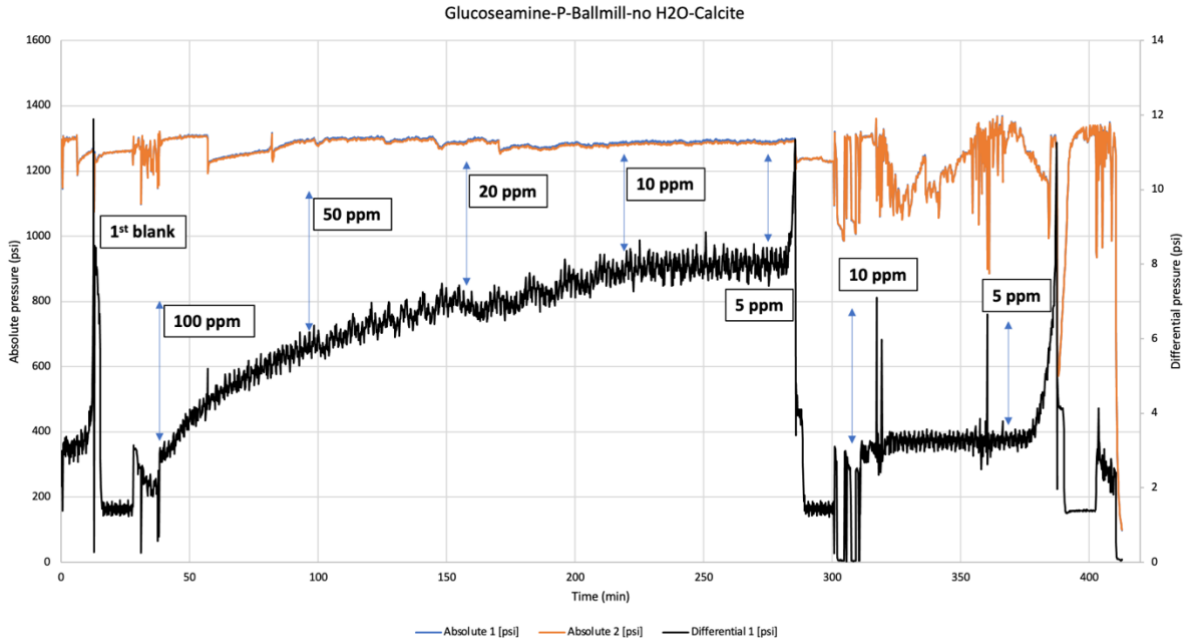

Figure 27: Differential pressure and time results from high-pressure dynamic tube blocking experiments of glucosamine-P-ballmill-No-H_2O against calcite scaling.

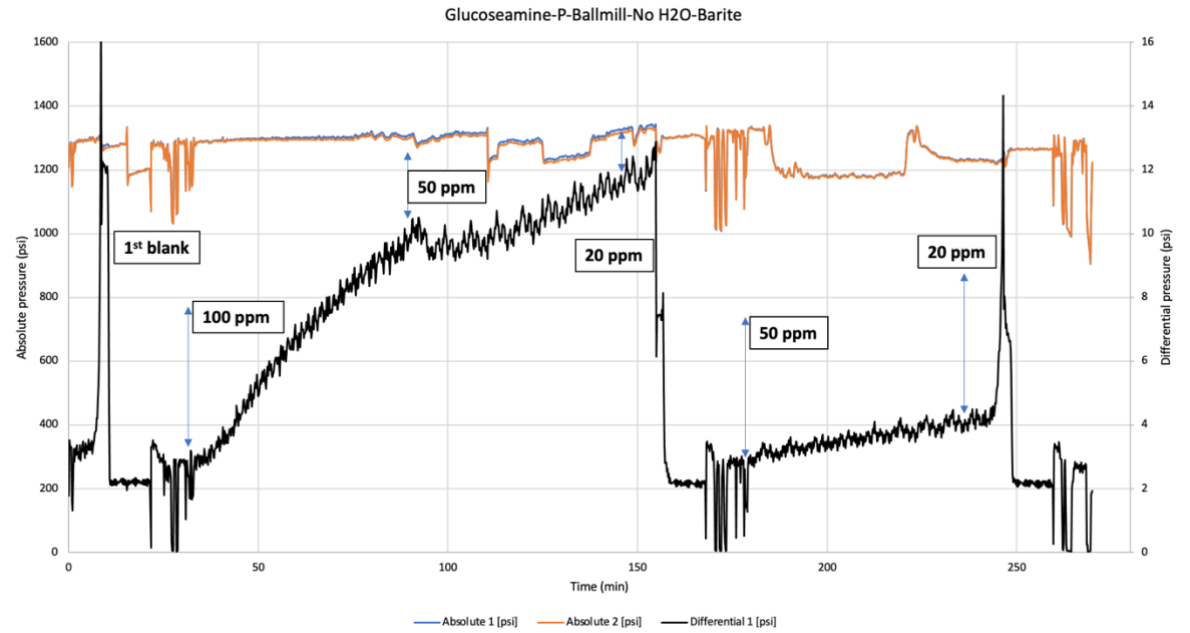

Figure 28: Differential pressure and time results from high-pressure dynamic tube blocking experiments of glucosamine-P-ballmill-No-H_2O against barite scaling.

From the scaling tests using the high-pressure dynamic tube blocking rig it was evident that ball milling without H_2O gave better results than with H_2O. However, because glucosamine-P-ballmill-No H_2O was not characterized from NMR, we could not know which product we have

tested on the rig. Although ball milling without H_2O resulted in better FIC values against both calcite and barite scale, ball milling with H_2O gave conclusive characterization, which was preferred. Thus, no further testing of glucosamine-P-ballmill-No H_2O were pursued. Glucosamine-P-ballmill-With H_2O still showed moderate calcite inhibition and poor barite inhibition. Indication of possible calcium incompatibility was observed in Figure 25. Therefore, a calcium compatibility test was performed on glucosamine-P-ballmill-With H_2O.

4.3.3. Calcium compatibility testing

The results for calcium compatibility testing of glucosamine-P-With H_2O are presented in Table 15. There was no sign of precipitation in any of the bottle tests, however, bottles with high dosages of SI were observed as opaque after one hour, four hours, and 24 hours.

Table 15: Calcium compatibility test of Glucosamine-P-ballmill-with H_2O with mixtures of Ca^{2+} concentrations (100, 1000, 10000) and SI concentrations (100, 1000, 10000, 50000).

SI	Ca^{2+} dose (ppm)	SI dose (ppm)	Appearance				
			After mixing	30 min	1 hour	4 hours	24 hours
Glucosamine-P-Ballmill-With H2O	100	100	Clear	Clear	Clear	Clear	Clear
		1000	Clear	Clear	Clear	Opaque	Opaque
		10000	Clear	Clear	Opaque	Opaque	Opaque
	1000	100	Clear	Clear	Clear	Clear	Clear
		1000	Clear	Clear	Clear	Opaque	Opaque
		10000	Clear	Clear	Opaque	Opaque	Opaque
	10000	100	Clear	Clear	Clear	Clear	Clear
		1000	Clear	Clear	Opaque	Opaque	Opaque
		10000	Clear	Clear	Opaque	Opaque	Opaque

An opaque solution does not mean a precipitate was formed, which could make squeeze treatment a possibility. However, squeeze treatment applications require a SI to withstand high temperatures. Degradation after long reflux times could suggest that glucosamine-P-ballmill-With H_2O cannot endure high temperatures. This would make it not applicable for squeeze treatment. Although this would have to be proven by a thermal stability test. On the other hand, glucosamine-P-ballmill-With H_2O could possibly endure high temperatures and keep the ring structure as the industrial way of making glucosamine involves boiling chitin in aqueous HCl (Einbu & Vårum, 2008; Gandhi & Laidler, n.d.). Nonetheless, if the thermal stability were to be poor, an option could be continuous injection topside.

4.3.4. Biodegradability

Biodegradability testing of glucosamine-P (4 hours reflux) using the OECD 306 method is presented in Table 16 along with a control flask containing sodium benzoate. The two most reliable Glucosamine-P bottles from biodegradability testing were 19.0% and 23.04%, which gave an average of 21.0%. The OSPAR regulations require a minimum of > 20% biodegradability of a SI. In this case, glucosamine-P fulfill these demands.

Table 16: Biodegradability testing of Glucosamine-P (4 hours reflux) using the OECD 306 method over 28 days.

SI/compound	Biodegradability by OECD 306 (%)
Sodium benzoate	80.14
Glucosamine-P	21

4.4. Further study

Further studies for glucosamine-P could be crystallization for a purer product to achieve improved scale inhibition and clearer NMR results. Synthesis of only one methylene phosphonate group could be an option to check if either biodegradability or scale inhibition would improve. Thermal stability testing could be done to check if glucosamine-P is thermally stable at high temperatures. If thermal stability tests were promising, this could make squeeze treatment applications an option. Also, observations after high temperature testing could give insight if the ring structure would be opened or not.

5. Conclusion

The synthesis of new classes of SIs was done by the addition of methylene phosphonate functional groups via the Moedtritzi-Irani method to yield efficient scale inhibition to starting materials claimed to have good biodegradability. Project A involved phosphonation of one, two and three methylene phosphonate groups to TSIDS (claimed to have good biodegradability), and the related chemicals TSEDAS, and DETAS, respectively. Project B involved the phosphonation of glucosamine, which was based on a published paper on PCH. Table 17 displays a summary of the results from SI testing of inhibition performance against calcite and barite scaling, calcium compatibility, and biodegradability in seawater (OECD306 BOD28).

Table 17: Summary of results from SI testing.

SI	Calcite inhibition	Barite inhibition	Calcium compatibility	Biodegradability in seawater (%)
TSIDS-P	Moderate	Poor	Moderate	72.56
TSEDAS-P	Excellent	Poor	Excellent	2.68
DETAS-P	Poor	Poor	N/A	N/A
Glucosamine-P-Ballmill-With H_2O	Moderate	Poor	Great	21.0

All synthesized SIs displayed poor barite inhibition. TSIDS-P showed exceptional biodegradability in seawater making it readily biodegradable by the OSPAR regulations for oilfield chemicals. A Ca-SI complex was made at high concentrations of SI for calcium compatibility testing which would make squeeze treatments challenging. However, TSIDS-P could be used for continuous injection topside if Ca^{2+} concentrations are moderate to low. TSEDAS-P displayed excellent calcium inhibition and excellent calcium compatibility making it viable for downhole squeeze treatment applications. However, due to low biodegradability in seawater, the SI would not be considered readily biodegradable. DETAS-P displayed poor performance for calcite inhibition. Since the SI was only partially soluble, the project was not pursued further. Glucosamine-P-Ballmill-With H_2O showed great calcium compatibility with only some cloudiness to the solution at high concentrations of SI and Ca^{2+}. Therefore, it could be used in squeeze treatment applications downhole. When tested for seawater biodegradability, the result was 21% biodegradability.

6. References

Adegoke, S. O., Falode, O. A., & Nwankwo, P. C. (2021). *Understanding oilfield scale deposition and inhibition mechanisms for optimum management: A review*. SPE Nigeria Annual International Conference and Exhibition. https://doi.org/10.2118/207133-MS

Almubarak, T., Ng, J. H., & Nasr-El-Din, H. (2017). *A Review of the corrosivity and degradability of aminopolycarboxylic acids*. Offshore Technology Conference. https://doi.org/10.4043/27535-MS

Al-Roomi, Y. M., & Hussain, K. F. (2016). Potential kinetic model for scaling and scale inhibition mechanism. *Desalination*, *393*, 186–195. https://doi.org/10.1016/j.desal.2015.07.025

Bageri, B. S., Mahmoud, M. A., Shawabkeh, R. A., Al-Mutairi, S. H., & Abdulraheem, A. (2017). Toward a Complete Removal of Barite (Barium Sulfate BaSO 4) Scale Using Chelating Agents and Catalysts. *Arabian Journal for Science and Engineering*, *42*(4), 1667–1674. https://doi.org/10.1007/s13369-017-2417-2

Baker Hughes - Legacy. (2013). *Scale inhibitor squeeze application*. https://www.youtube.com/watch?v=lTvtJcd8L8Y

Binmerdhah, A., & Yassin, A. (2007). *Study of scale formation in oil reservoir during water injection-A review*.

Boethling, R. S., Sommer, E., & DiFiore, D. (2007). Designing small molecules for biodegradability. *Chemical Reviews*, *107*(6), 2207–2227. https://doi.org/10.1021/cr050952t

Chillingar, G. V., Mourhatch, R., & Al-Qahtani, A. (2008). *The Fundamentals of Corrosion and Scaling for Petroleum and Environmental Engineers*. Austin: Gulf publishing company. https://books.google.com/books/about/The_Fundamentals_of_Corrosion_and_Scalin.html?hl=no&id=rQxBAQAAQBAJ

Dyer, S. J., Anderson, C. E., & Graham, G. M. (2004). Thermal stability of amine methyl phosphonate scale inhibitors. *Journal of Petroleum Science and Engineering*, *43*(3), 259–270. https://doi.org/10.1016/j.petrol.2004.02.018

Einbu, A., & Vårum, K. M. (2008). Characterization of chitin and its hydrolysis to GlcNAc and GlcN. *Biomacromolecules*, *9*(7), 1870–1875. https://doi.org/10.1021/bm8001123

Fink, J. (2021a). Scale inhibitors. In *Petroleum engineer's guide to oil field chemicals and fluids*. (third edition, pp. 351–391). Gulf Professional Publishing.

Fink, J. (2021b). Scale inhibitors. In *Petroleum engineer's guide to oil field chemicals and fluids*. (3rd ed., pp. 351–391). Gulf Professional Publishing. https://doi.org/10.1016/B978-0-323-85438-2.00007-4

Frenier, Wayne. W., & Ziauddin, M. (2008a). *Formation, removal, and inhibition of inorganic scale in the oilfield environment* (Nicholas. A. Wolf & Ryan. A. Hartman, Eds.). Society of petroleum engineers.

Frenier, Wayne. W., & Ziauddin, M. (2008b). Inhibition of inorganic scale formation. In Nicholas. A. Wolf & Ryan. A. Hartman (Eds.), *Formation, removal, and inhibition of inorganic scale in the oilfield environment* (pp. 87–88). Society of petroleum engineers.

Frenier, Wayne. W., & Ziauddin, M. (2008c). Inorganic scales found in the oil field. In Nicholas. A. Wolf & Ryan. A. Hartman (Eds.), *Formation, removal, and inhibition of inorganic scale in the oilfield environment* (pp. 22–49). Society of petroleum engineers.

Gandhi, N., & Laidler, J. K. (n.d.). *Preparation of glucosamine hydrochloride* (Alberta Research Council Inc. Patent No. United States Patent 6486307). https://patentimages.storage.googleapis.com/33/62/1a/26712ef78450ed/US6486307.pdf

Graham, G. M., Dyer, S. J., & Shell, P. S. (2000). *Potential Application Of Amine Methylene Phosphonate Based Inhibitor Species In HP/HT Environments For Improved Carbonate Scale Inhibitor Performance*. International Symposium on Oilfield Scale. https://doi.org/10.2118/60217-MS

Graham, G. M., Jordan, M. M., Graham, G. C., Sablerolle, W., Sorbie, K. S., Hill, P., & Bunney, J. (1997). *The Implication of HP/HT Reservoir Conditions on the Selection and Application of Conventional Scale Inhibitors: Thermal Stability Studies*. International Symposium on Oilfield Chemistry. https://doi.org/10.2118/37274-MS

Hasson, D., Shemer, H., & Sher, A. (2011). State of the art of friendly "green" scale control inhibitors: A review article. *Industrial & Engineering Chemistry Research*, *50*(12), 7601–7607. https://doi.org/10.1021/ie200370v

Hustad, B. M., Svela, O. G., Olsen, J. H., Ramstad, K., & Tjomsland, T. (2012). *Downhole Chemical Injection Lines - Why Do They Fail? Experiences, Challenges and Application of New Test Methods*. SPE International Conference on Oilfield Scale. https://doi.org/10.2118/154967-MS

Jafar Mazumder, M. A. (2020). A review of green scale inhibitors: Process, types, mechanism and properties. *Coatings*, *10*(10), 928. https://doi.org/10.3390/coatings10100928

Jarrahian, K., Sorbie, K., Singleton, M., Boak, L., & Graham, A. (2019). *Building a fundamental understanding of scale inhibitor retention in carbonate formations*. SPE International Conference on Oilfield Chemistry. https://doi.org/10.2118/193635-MS

Jensen, M. K., & Kelland, M. A. (2012). A new class of hyperbranched polymeric scale inhibitors. *Journal of Petroleum Science and Engineering*, *94–95*, 66–72. https://doi.org/10.1016/j.petrol.2012.06.025

Ji, Y., Chen, Y., Le, J., Qian, M., Huan, Y., Yang, W., Yin, X., Liu, Y., Wang, X., & Chen, Y. (2017). Highly effective scale inhibition performance of amino trimethylenephosphonic acid on calcium carbonate. *Desalination*, *422*, 165–173. https://doi.org/10.1016/j.desal.2017.08.027

Jordan, M. M., Sorbie, K. S., Griffin, P., Hennessey, S., Hourston, K. E., & Waterhouse, P. (1995). *Scale inhibitor adsorption/desorption vs. precipitation: The potential for extending squeeze life while minimising formation damage*. SPE European Formation Damage Conference. https://doi.org/10.2118/30106-MS

Jordan, M. M., Sorbie, K. S., Yuan, M. D., Taylor, K., Hourston, K. E., Ramstad, K., & Griffin, P. (1995). *Static and dynamic adsorption of phosphonate and polymeric scale inhibitors onto reservoir core from laboratory tests to field application*. SPE International Symposium on Oilfield Chemistry. https://doi.org/10.2118/29002-MS

Kamal, M. S., Hussein, I., Mahmoud, M., Sultan, A. S., & Saad, M. A. S. (2018). Oilfield scale formation and chemical removal: A review. *Journal of Petroleum Science and Engineering*, *171*, 127–139. https://doi.org/10.1016/j.petrol.2018.07.037

Kan, A., Dai, Z., Mason, ·, Tomson, M., & Science, P. (2020). The state of the art in scale inhibitor squeeze treatment. *Petroleum Science*, *17*, 3. https://doi.org/10.1007/s12182-020-00497-z

Kelland, M. A. (2011). Effect of Various Cations on the Formation of Calcium Carbonate and Barium Sulfate Scale with and without Scale Inhibitors. *Industrial & Engineering Chemistry Research*, *50*(9), 5852–5861. https://doi.org/10.1021/ie2003494

Kelland, M. A. (2014a). Chemical scale removal. In *Prodution chemicals for the oil and gas industry* (second edition, pp. 83–88). CRC press.

Kelland, M. A. (2014b). Designing greener chemicals. In *Prodution chemicals for the oil and gas industry* (second edition, pp. 13–17). CRC press.

Kelland, M. A. (2014c). Environmental and ecotoxicological regulations. In *Prodution chemicals for the oil and gas industry* (second edition, pp. 9–10). CRC press.

Kelland, M. A. (2014d). Methods of deploying scale inhibitors. In *Prodution chemicals for the oil and gas industry* (second edition, pp. 71–80). CRC press.

Kelland, M. A. (2014e). Scale control. In *Prodution chemicals for the oil and gas industry* (second edition, p. 51). CRC press.

Kelland, M. A. (2014f). Scale inhibition of group II carbonates and sulfates. In *Production chemicals for the oil and gas industry* (second edition, pp. 56–69). CRC press.

Kelland, M. A. (2014g). Scale inhibitor squeeze treatments. In *Prodution chemicals for the oil and gas industry* (second edition, pp. 72–78). CRC press.

Kelland, M. A. (2014h). Types of scales. In *Prodution chemicals for the oil and gas industry* (second edition, pp. 51–55). CRC press.

Kezerian, C., & Ramsey, W. M. (n.d.). *Bis-adduction products and methods to prepare same* (Stauffer chemical CO Patent No. United States patent 3158635). https://patentimages.storage.googleapis.com/6b/e4/77/9adb9fdfb66aba/US3158635.pdf

Khormali, A., Petrakov, D. G., & Nazari Moghaddam, R. (2017). Study of adsorption/desorption properties of a new scale inhibitor package to prevent calcium carbonate formation during water injection in oil reservoirs. *Journal of Petroleum Science and Engineering*, *153*, 257–267. https://doi.org/10.1016/j.petrol.2017.04.008

Kumar, S., Naiya, T. K., & Kumar, T. (2018). Developments in oilfield scale handling towards green technology-A review. *Journal of Petroleum Science and Engineering*, *169*, 428–444. https://doi.org/10.1016/j.petrol.2018.05.068

Liu, Z., Sun, Y., Zhou, X., Wu, T., Tian, Y., & Wang, Y. (2011). Synthesis and scale inhibitor performance of polyaspartic acid. *Journal of Environmental Sciences*, *23*, S153–S155. https://doi.org/10.1016/S1001-0742(11)61100-5

Mady, M. F., Abdel-Azeim, S., & Kelland, M. A. (2021). Investigation of the Antiscaling Performance of Phosphonated Chitosan for Upstream Petroleum Industry Application. *ACS Sustainable Chemistry & Engineering*, *9*(48), 16494–16505. https://doi.org/10.1021/acssuschemeng.1c06786

Mady, M. F., Bagi, A., & Kelland, M. A. (2016). Synthesis and Evaluation of New Bisphosphonates as Inhibitors for Oilfield Carbonate and Sulfate Scale Control. *Energy & Fuels*, *30*(11), 9329–9338. https://doi.org/10.1021/acs.energyfuels.6b02117

Mady, M. F., Bayat, P., & Kelland, M. A. (2020). Environmentally friendly phosphonated polyetheramine scale inhibitors—Excellent calcium compatibility for oilfield applications. *Industrial & Engineering Chemistry Research*, *59*(21), 9808–9818. https://doi.org/10.1021/acs.iecr.0c01636

Mady, M. F., Fevang, S., & Kelland, M. A. (2019). Study of Novel Aromatic Aminomethylenephosphonates as Oilfield Scale Inhibitors. *Energy & Fuels*, *33*(1), 228–237. https://doi.org/10.1021/acs.energyfuels.8b03531

Mady, M. F., & Kelland, M. A. (2017). Overview of the Synthesis of Salts of Organophosphonic Acids and Their Application to the Management of Oilfield Scale. *Energy & Fuels*, *31*(5), 4603–4615. https://doi.org/10.1021/acs.energyfuels.7b00708

Mady, M. F., Malmin, H., & Kelland, M. A. (2019). Sulfonated nonpolymeric aminophosphonate scale inhibitors—Improving the compatibility and biodegradability. *Energy & Fuels*, *33*(7), 6197–6204. https://doi.org/10.1021/acs.energyfuels.9b01032

Mady, M. F., Ortega, R., & Kelland, M. A. (2022). Exploring Modified Alendronic Acid as a New Inhibitor for Calcium-Based Oilfield Scales. *Energy & Fuels*, *36*(4), 1863–1873. https://doi.org/10.1021/acs.energyfuels.1c03936

Merdhah, A. B. B., & Yassin, A. A. M. (2009). Laboratory Study on Precipitation of Barium Sulphate in Malaysia Sandstone Cores. *The Open Petroleum Engineering Journal*, *2*(1). https://benthamopen.com/ABSTRACT/TOPEJ-2-1

Mpelwa, M., & Tang, S.-F. (2019). State of the art of synthetic threshold scale inhibitors for mineral scaling in the petroleum industry: A review. *Petroleum Science*, *16*(4), 830–849. https://doi.org/10.1007/s12182-019-0299-5

Norwegian oil and gas association. (2017). *Environmental report 2017*. https://www.norskoljeoggass.no/contentassets/b3bdff43b7ef4c4da10c7db1f3b782e4/environmental-report-2017.pdf

Olajire, A. A. (2015). A review of oilfield scale management technology for oil and gas production. *Journal of Petroleum Science and Engineering*, *135*, 723–737. https://doi.org/10.1016/j.petrol.2015.09.011

Ott, A., Martin, T. J., Whale, G. F., Snape, J. R., Rowles, B., Galay-Burgos, M., & Davenport, R. J. (2019). Improving the biodegradability in seawater test (OECD 306). *Science of The Total Environment*, *666*, 399–404. https://doi.org/10.1016/j.scitotenv.2019.02.167

Shaughnessy, C. M., & Kline, W. E. (1983). EDTA Removes Formation Damage at Prudhoe Bay. *Journal of Petroleum Technology*, *35*(10), 1783–1791. https://doi.org/10.2118/11188-PA

Tantayakom, V., Fogler, H. S., Charoensirithavorn, P., & Chavadej, S. (2005). Kinetic study of scale inhibitor precipitation in squeeze treatment. *Crystal Growth & Design*, *5*(1), 329–335. https://doi.org/10.1021/cg049874d

Tomson, M. B., Fu, G., Watson, M. A., & Kan, A. T. (2003). Mechanisms of Mineral Scale Inhibition. *SPE Production & Facilities*, *18*(03), 192–199. https://doi.org/10.2118/84958-PA

Vazquez, O., Fursov, I., & Mackay, E. (2016). Automatic optimization of oilfield scale inhibitor squeeze treatment designs. *Journal of Petroleum Science and Engineering*, *147*, 302–307. https://doi.org/10.1016/j.petrol.2016.06.025

Veisi, M., Johnson, S., Shafer-Peltier, K., Liang, J.-T., Berkland, C., Chen, M., & Barati, R. (2019). Controlled release of poly (vinyl sulfonate) scale inhibitor to extend reservoir treatment lifetime. *Journal of Applied Polymer Science*, *136*(12), 47225. https://doi.org/10.1002/app.47225

Wennberg, A. C., Petersen, K., & Grung, M. (2017). *Biodegradation of selected offshore chemicals* (p. 118) [Environmental report]. Norwegian institute for water research, NIVA. https://www.miljodirektoratet.no/globalassets/publikasjoner/m911/m911.pdf

Zeng, J.-P., Wang, F.-H., & Gong, X.-D. (2013). Molecular dynamics simulation of the interaction between polyaspartic acid and calcium carbonate. *Molecular Simulation*, *39*(3), 169–175. https://doi.org/10.1080/08927022.2012.709632

Zhang, P., Liu, Y., Zhang, N., Ip, W. F., Kan, A. T., & Tomson, M. B. (2019). A novel attach-and-release mineral scale control strategy: Laboratory investigation of retention and release of scale inhibitor on pipe surface. *Journal of Industrial and Engineering Chemistry*, *70*, 462–471. https://doi.org/10.1016/j.jiec.2018.11.009

Zotzmann, J., Vetter, A., & Regenspurg, S. (2018). Evaluating efficiency and stability of calcite scaling inhibitors at high pressure and high temperature in laboratory scale. *Geothermal Energy*, *6*(1), 18. https://doi.org/10.1186/s40517-018-0105-4

Appendix A

Scale inhibitor solution

Scale inhibitor solution procedure:

1. The original amount measured for the reaction will be in a 0.5g SI solution. Measure the amount of solution present after the reflux reaction in mL.
2. Calculate the amount of SI solution needed by following the formula and add to a beaker. $\frac{SI\ solution\ measured\ (mL)}{Original\ amount\ (g)} * 0.5g = SI\ solution\ for\ scale\ test$
3. After the amount of SI solution needed is calculated, we take this amount and subtract it from 500 mL of deionized water. $500\ mL - SI\ solution\ (mL) = Amount\ deionized\ water\ water$
4. Add the calculated amount of DI water to the same beaker.

1% solutions for BOD28 test

Calculations for base chemical solutions

0.1g of active sample was needed.

$$\frac{0.1g}{weight\ percent\ of\ base\ chemical} = active\ sample\ (0.1g) + water\ weight\ (rest\ of\ weight)$$

We wanted a 10 mL 1% solution. This was achieved by following the following calculations.

$$9.99g + 0.1g \rightarrow \frac{0.1g}{9.9g + 0.1g} * 100\% = 1wt\%$$

$$9.9g - water\ weight\ of\ base\ chemical = weight\ of\ deionized\ water$$

Finally, $(active\ sample + water\ weight) + Deionized\ water = 10mL\ 1wt\%\ solution$

Calculations for phosphonated solutions

Firstly, the volume of the phosphonated solution was measured. Then to measure how much of our base chemical was left, this calculation was made.

$$Initial\ base\ chemical\ weight - amount\ used\ in\ SI\ solution = Base\ chemical\ left$$

This gave us Base chemical left in Volume of phosphonated solution.

$$0.1g \rightarrow \frac{Volume\ SI\ solution}{Base\ chemical\ left} * 0.1g = Volume\ (active\ sample\ (0.1g) + water\ weight)$$

The Volume (active sample (0.1g) + water weight) was transferred to a 10 mL vile and weighed in grams.

$$9.9g - water\ weight = weight\ of\ deionized\ water$$

Finally, $(active\ sample + water\ weight) + Deionized\ water = 10mL\ 1wt\%\ solution$

EDTA cleaning solution procedure

Table 18: Components used to make EDTA solution.

Chemical formula	**g/2L**
NaOH	40.0
Na2EDTA*H_2O	120.0

1. From table 8 (above), measure 40.0g NaOH in a beaker. Tare the weight and measure 120.0g Na2EDTA*2H_2O in the same beaker.
2. Dissolve in 2L deionized water.
3. Finally, degas the EDTA solution for 15-20min.

Appendix B

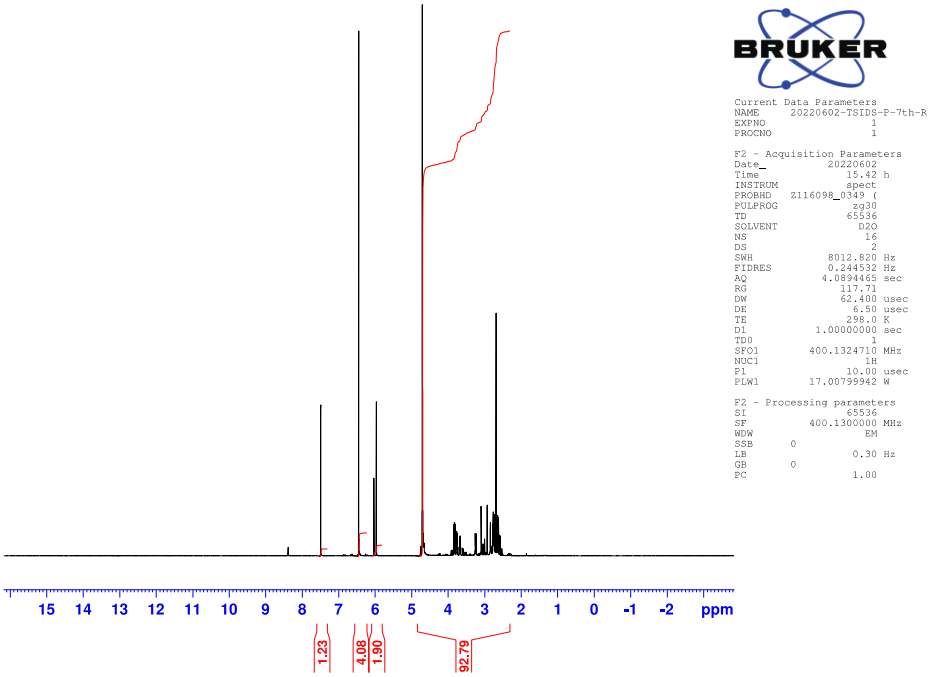

Figure 29: [1]H NMR for TSIDS-P.

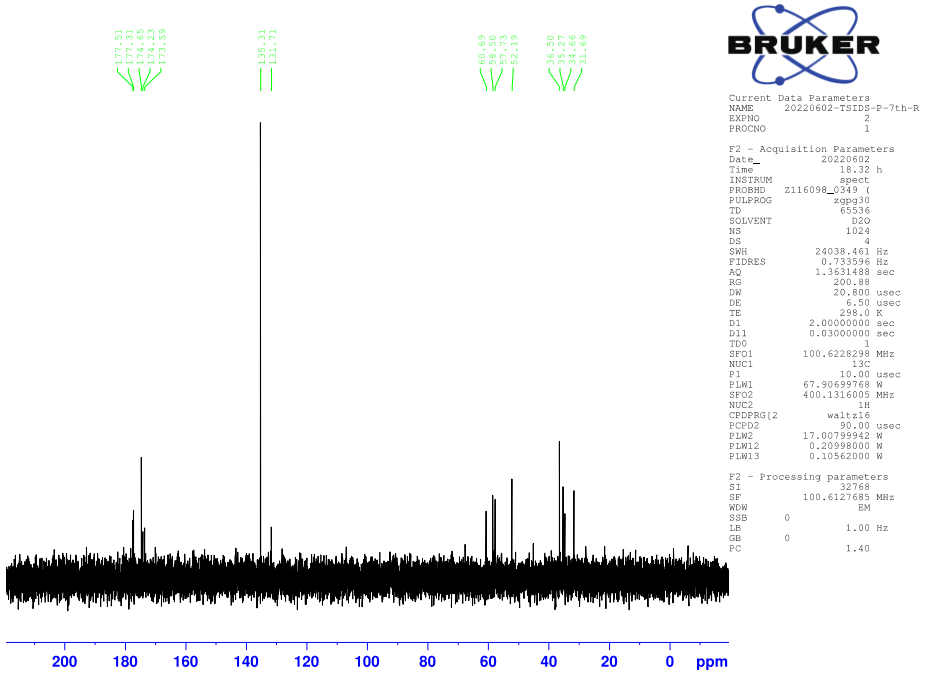

Figure 30: [13]C NMR for TSIDS-P.

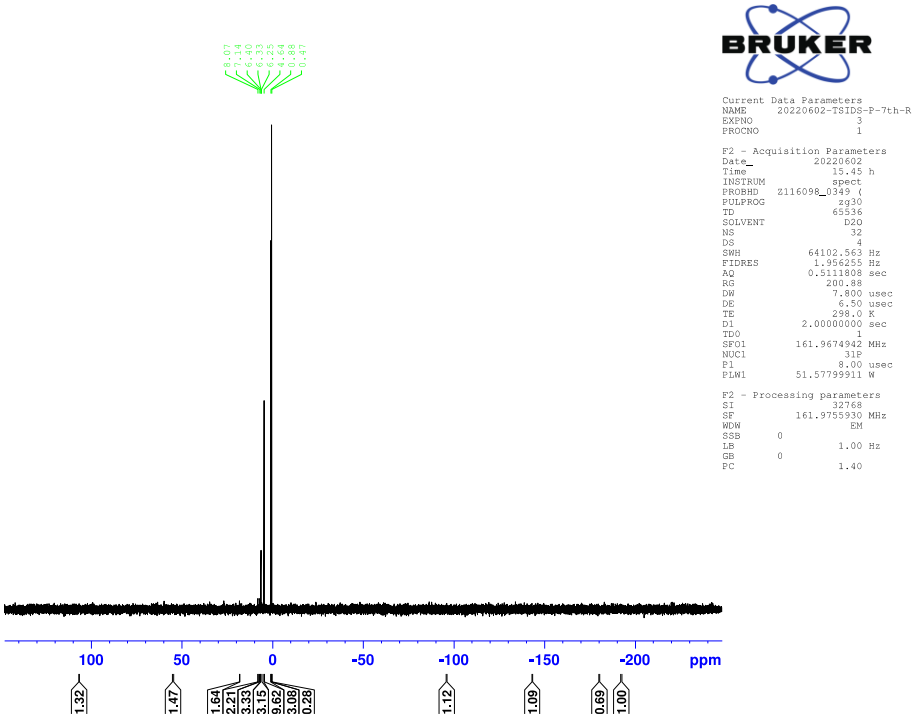

Figure 31: ^{31}P NMR with coupling for TSIDS-P.

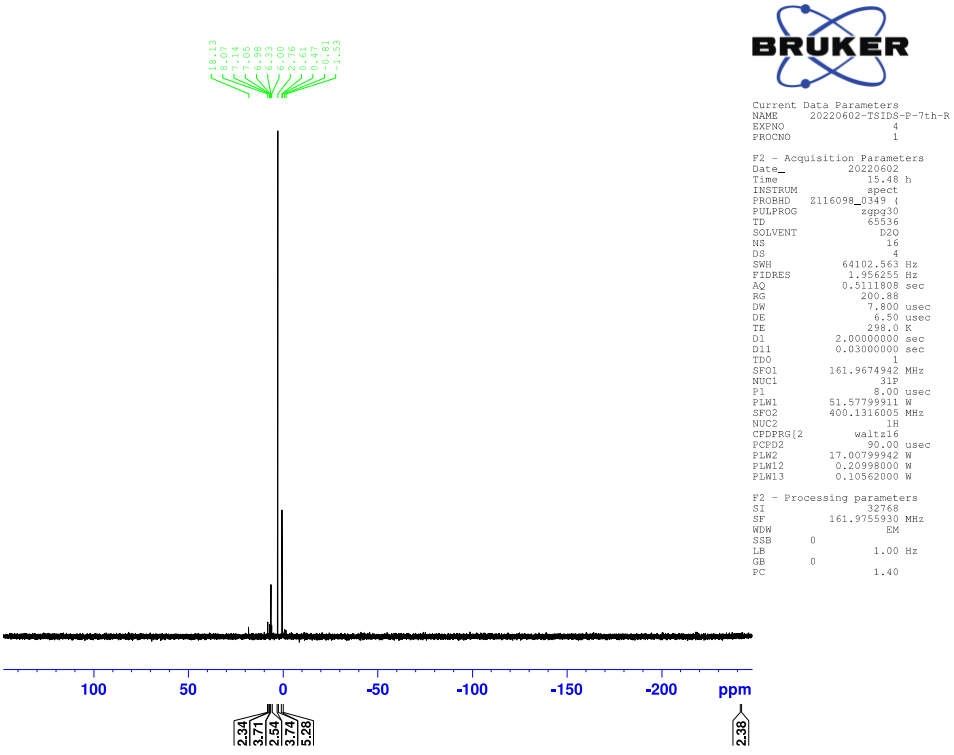

Figure 32: ^{31}P NMR with decoupling for TSIDS-P.

Appendix C

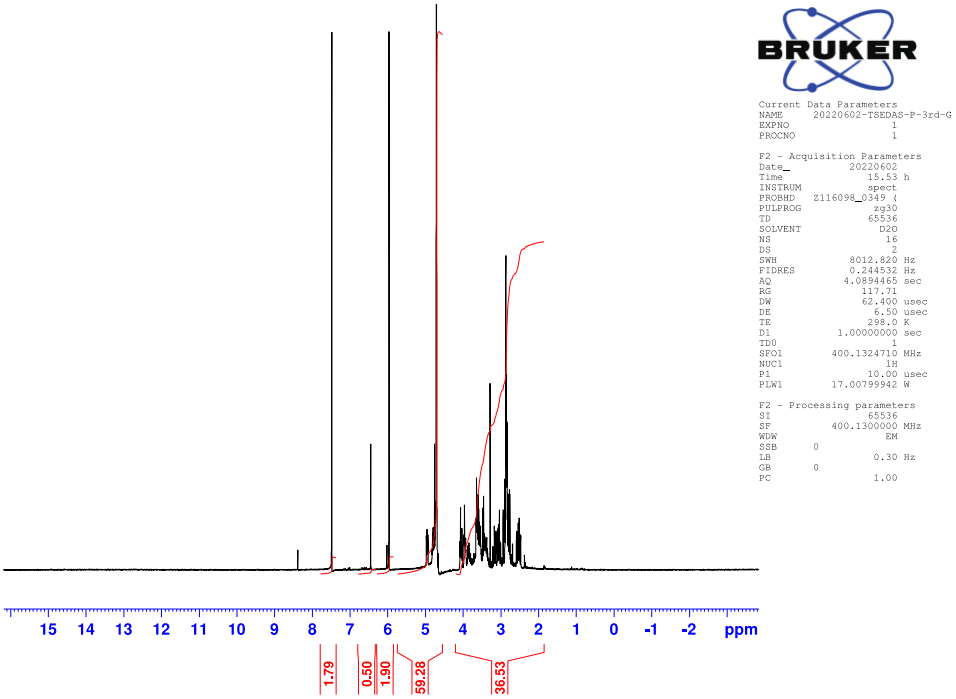

Figure 33: [1]H NMR for TSEDAS-P.

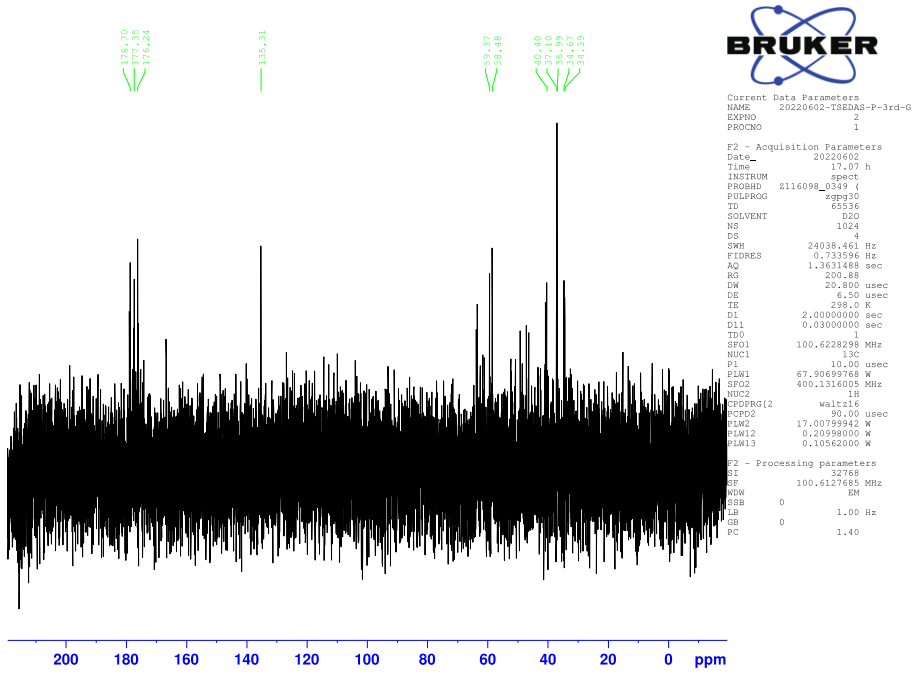

Figure 34: [13]C NMR for TSEDAS-P.

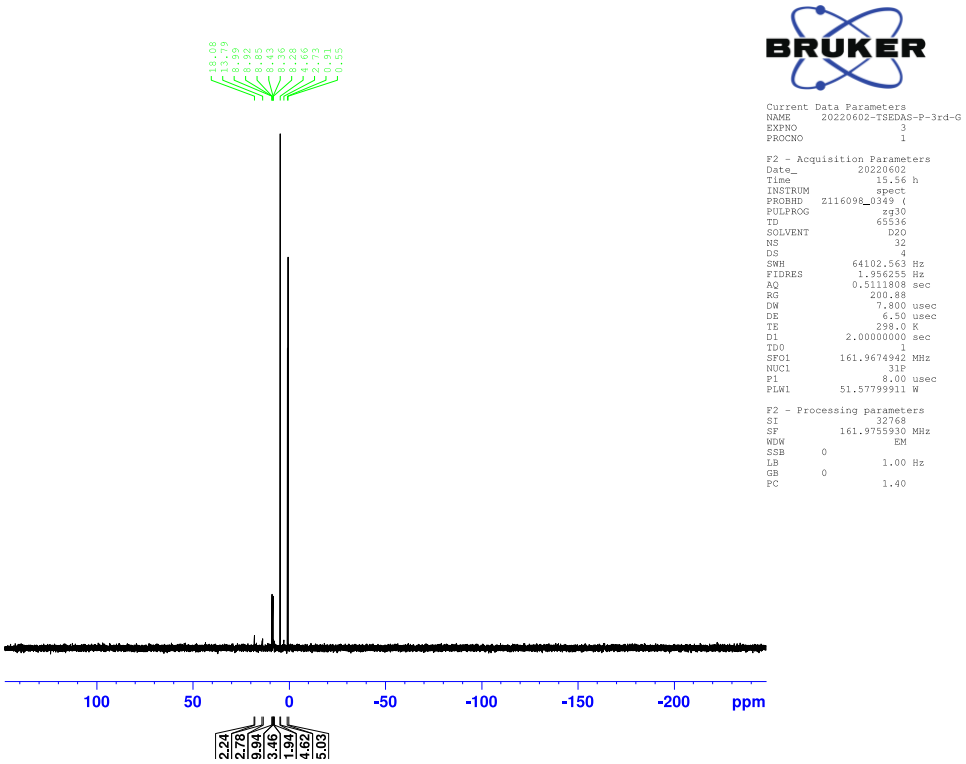

BRUKER

```
Current Data Parameters
NAME      20220602-TSEDAS-P-3rd-G
EXPNO                 3
PROCNO                1

F2 - Acquisition Parameters
Date_           20220602
Time              15.56 h
INSTRUM           spect
PROBHD   Z116098_0349 (
PULPROG           zg30
TD               65536
SOLVENT           D2O
NS                 32
DS                  4
SWH           64102.563 Hz
FIDRES         1.956255 Hz
AQ            0.5111808 sec
RG               200.88
DW                7.800 usec
DE                6.50 usec
TE               298.0 K
D1            2.00000000 sec
TD0                1
SFO1        161.9674942 MHz
NUC1              31P
P1                8.00 usec
PLW1        51.57799911 W

F2 - Processing parameters
SI                32768
SF          161.9755930 MHz
WDW               EM
SSB       0
LB                1.00 Hz
GB        0
PC                1.40
```

Figure 35: ^{31}P NMR with coupling for TSEDAS-P.

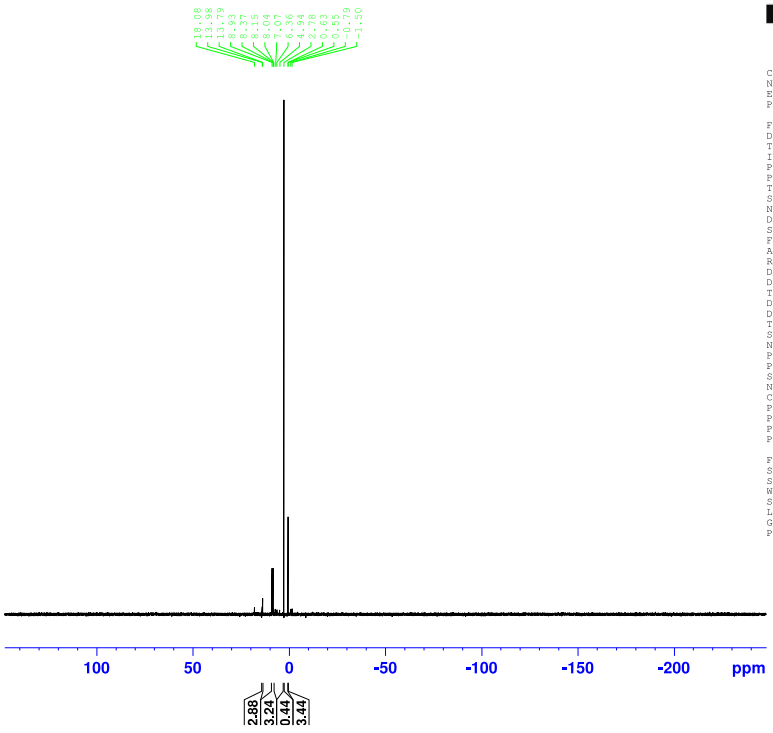

BRUKER

```
Current Data Parameters
NAME      20220602-TSEDAS-P-3rd-G
EXPNO                 4
PROCNO                1

F2 - Acquisition Parameters
Date_           20220602
Time              16.00 h
INSTRUM           spect
PROBHD   Z116098_0349 (
PULPROG          zgpg30
TD               65536
SOLVENT           D2O
NS                 16
DS                  4
SWH           64102.563 Hz
FIDRES         1.956255 Hz
AQ            0.5111808 sec
RG               200.88
DW                7.800 usec
DE                6.50 usec
TE               298.0 K
D1            2.00000000 sec
D11           0.03000000 sec
TD0                1
SFO1        161.9674942 MHz
NUC1              31P
P1                8.00 usec
PLW1        51.57799911 W
SFO2        400.1316005 MHz
NUC2               1H
CPDPRG[2         waltz16
PCPD2             90.00 usec
PLW2        17.00799942 W
PLW12        0.20998000 W
PLW13        0.10562000 W

F2 - Processing parameters
SI                32768
SF          161.9755930 MHz
WDW               EM
SSB       0
LB                1.00 Hz
GB        0
PC                1.40
```

Figure 36: ^{31}P NMR with decoupling for TSEDAS-P.

Appendix D

Glucosamine-P reflux (4 hours)

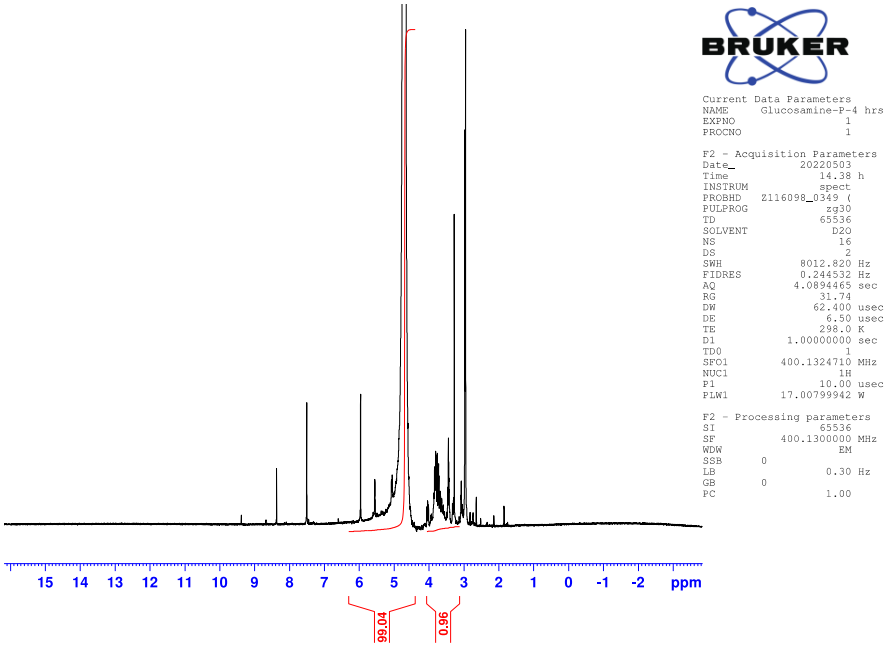

Figure 37: [1]H NMR for Glucosamine-P-reflux (4 hours).

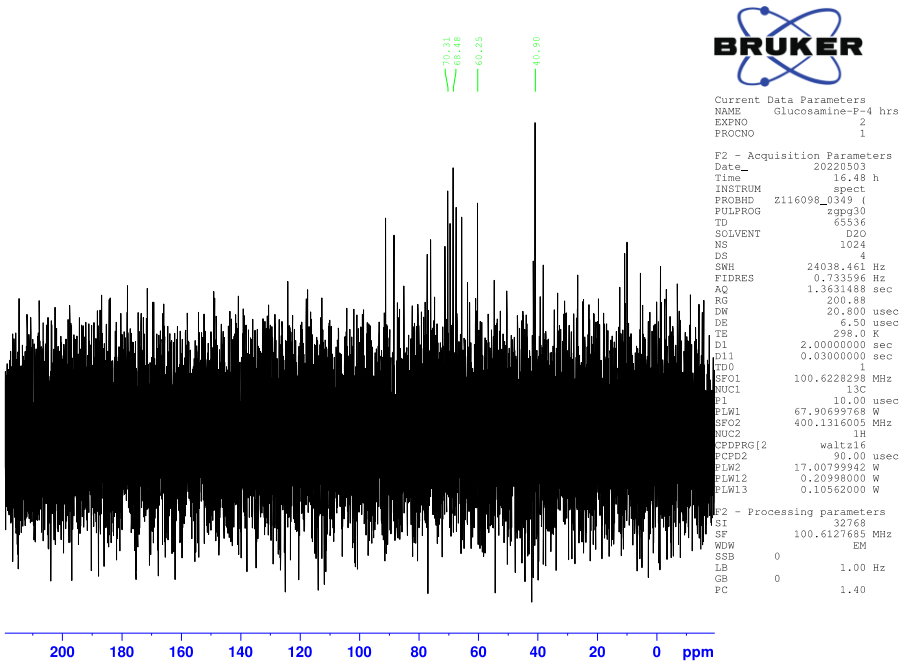

Figure 38: [13]C NMR for glucosamine-P-reflux (4 hours).

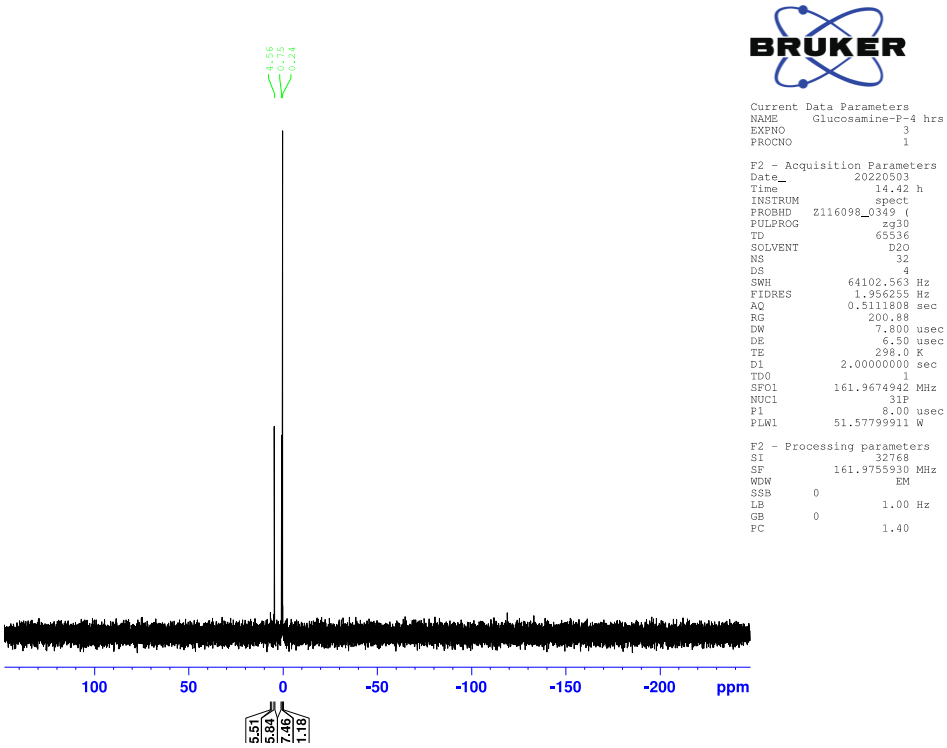

Figure 39: ^{31}P NMR with coupling for glucosamine-P-reflux (4 hours).

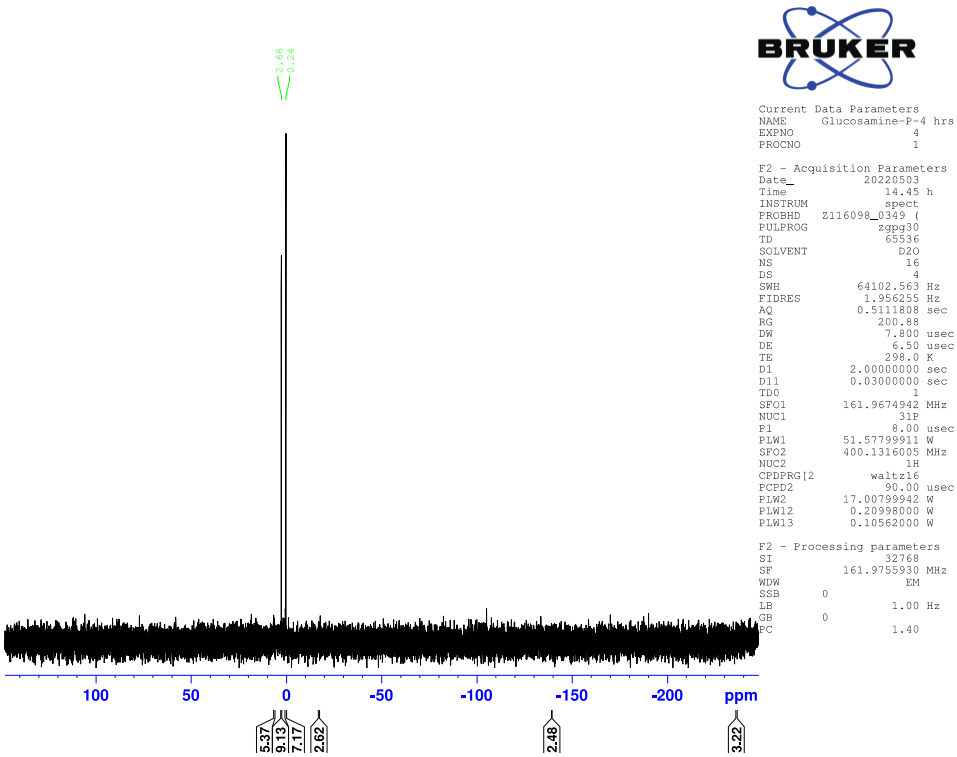

Figure 40: ^{31}P NMR with decoupling for glucosamine-P-reflux (4 hours).

Glucosamine-P reflux (8 hours)

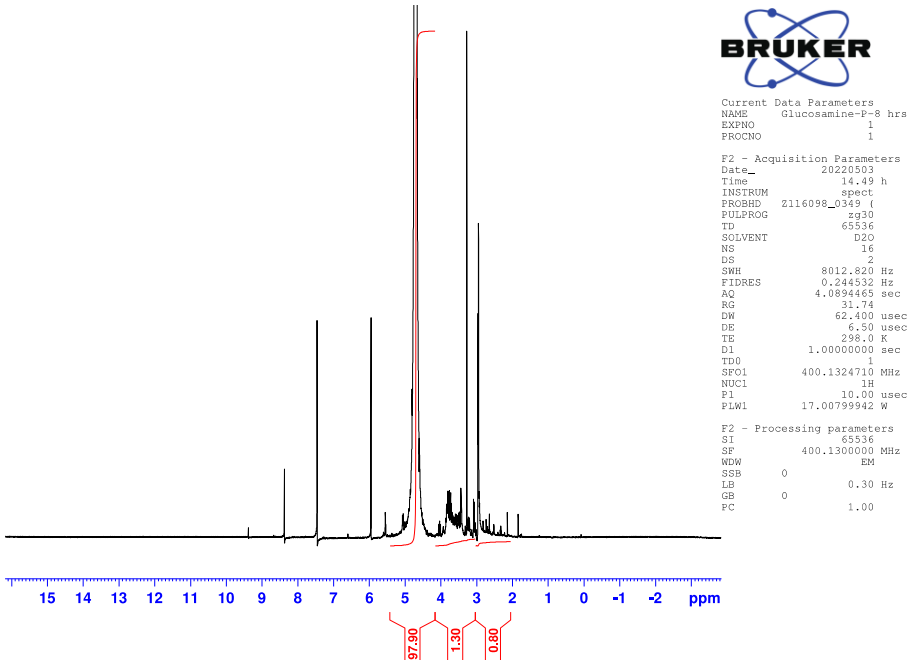

Figure 41: ^{1}H NMR for glucosamine-P-reflux (8 hours).

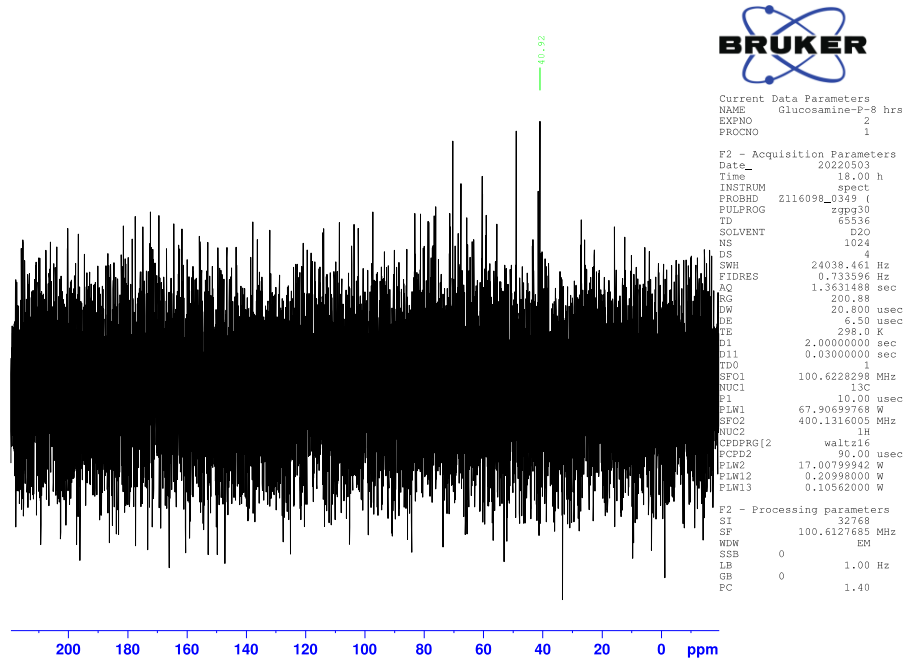

Figure 42: ^{13}C NMR for glucosamine-P-reflux (8 hours).

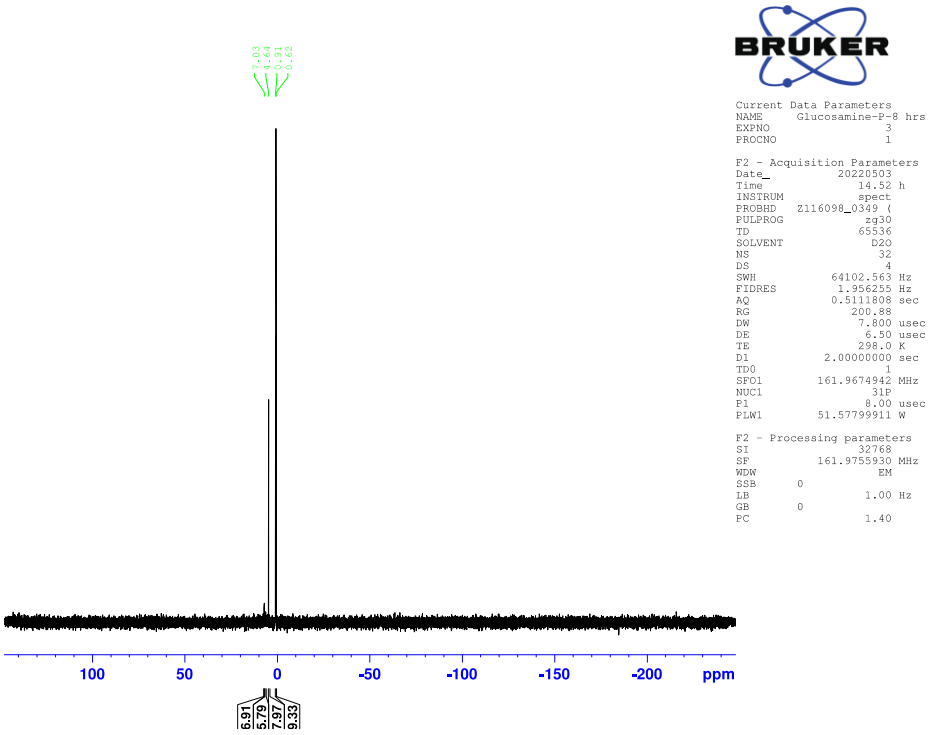

Figure 43: ^{31}P NMR for glucosamine with coupling.

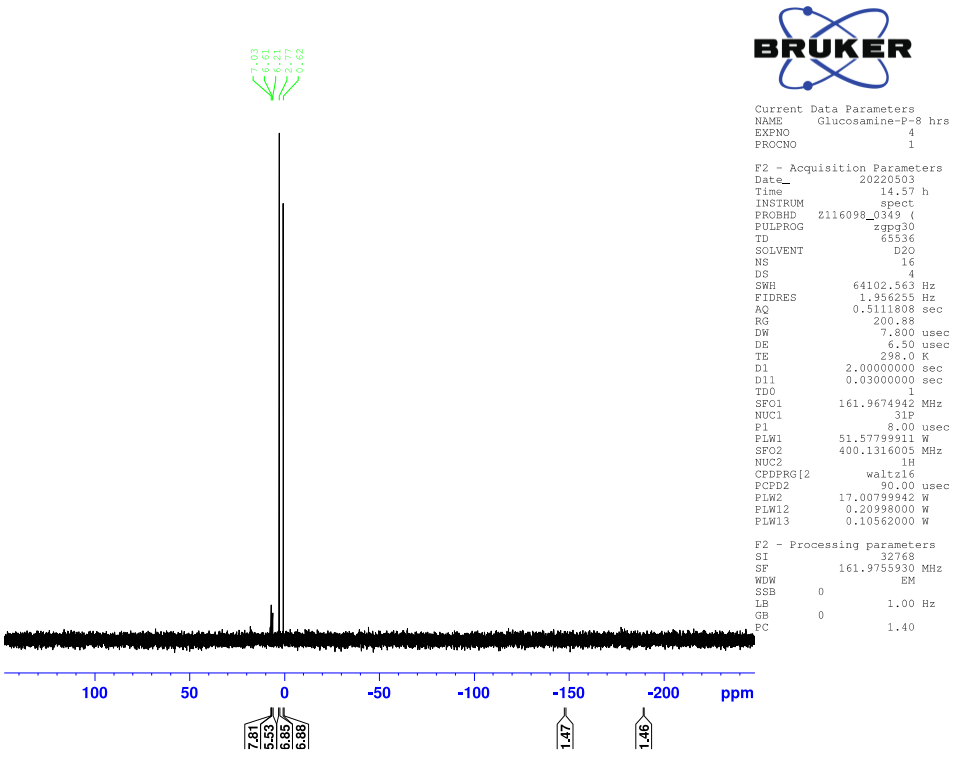

Figure 44: ^{31}P NMR with decoupling for glucosamine-P-reflux (8 hours).

Glucosamine-P-Ballmill-With H_2O

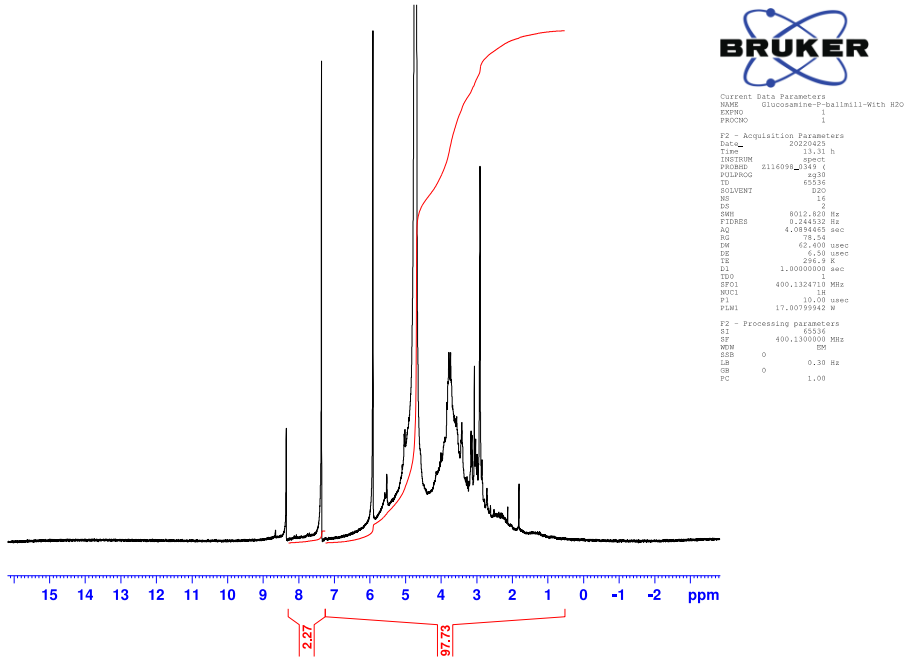

Figure 45: ^{1}H NMR for glucosamine-P-Ballmill-With H_2O.

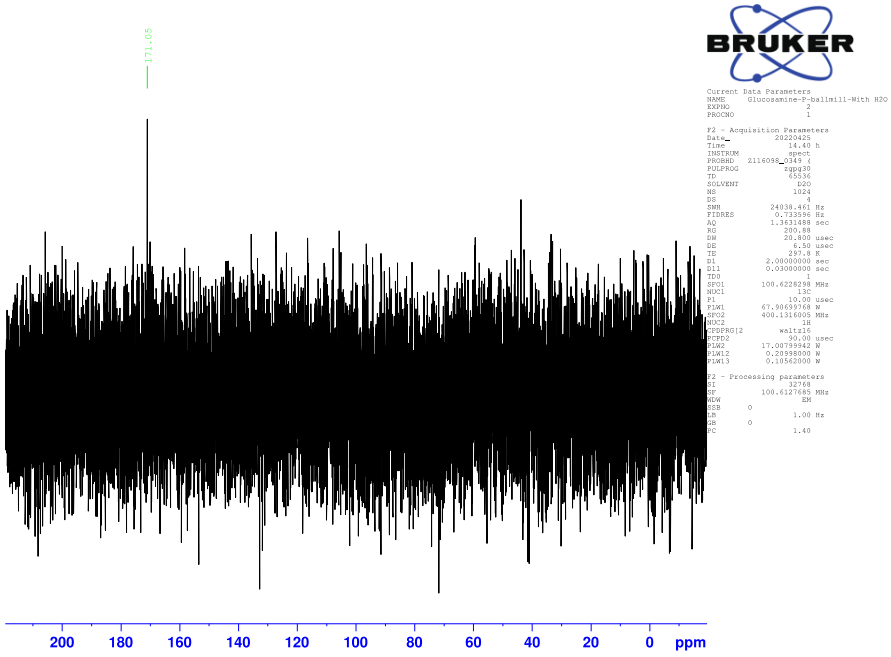

Figure 46: ^{13}C NMR for glucosamine-P-Ballmill-With H_2O.

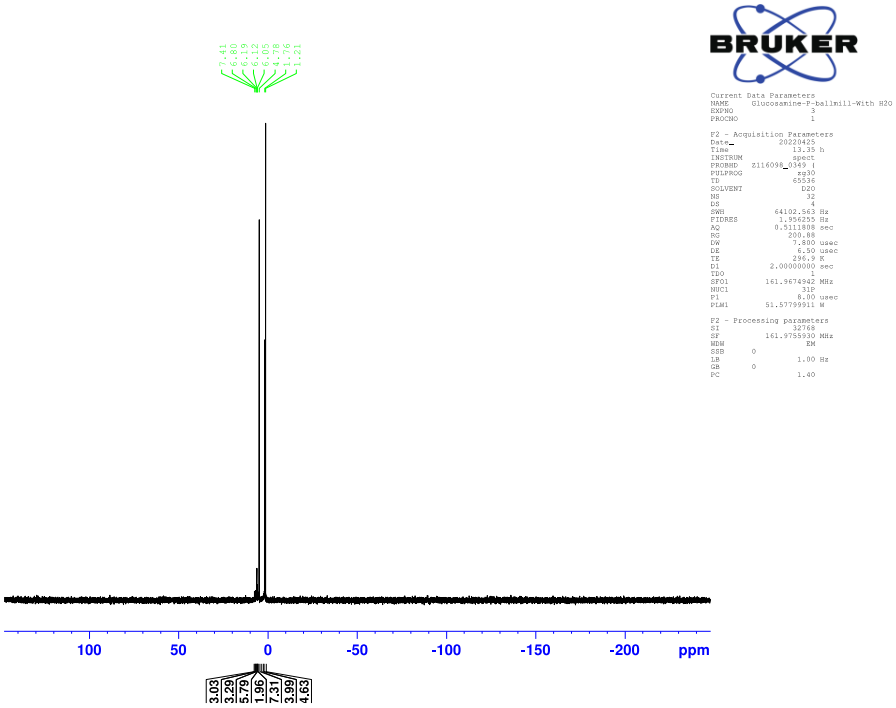

Figure 47: ^{31}P NMR with coupling for glucosamine-P-Ballmill-With H_2O.

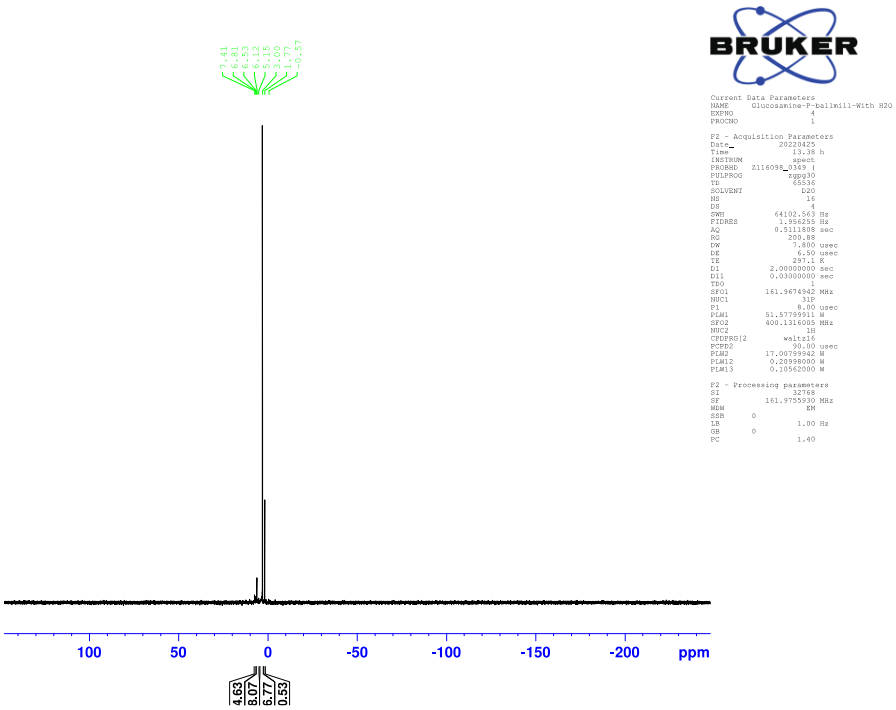

Figure 48: ^{31}P with decoupling for glucosamine-P-Ballmill-With H_2O.

Glucosamine-P-Ballmill-No H_2O

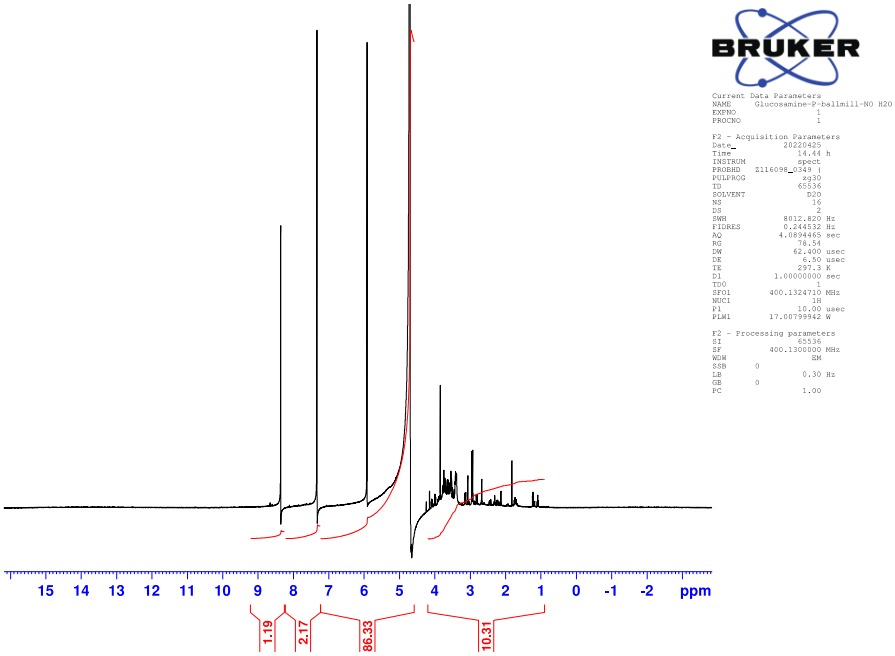

Figure 49: ^{1}H NMR for glucosamine-P-Ballmill-No H_2O.

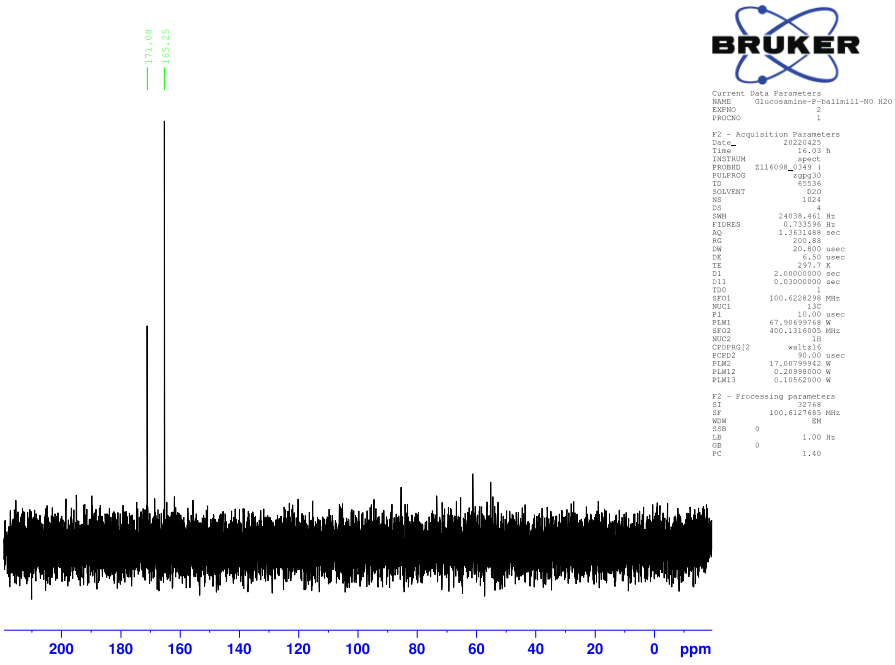

Figure 50: ^{13}C NMR for glucosamine-P-Ballmill-No H_2O.

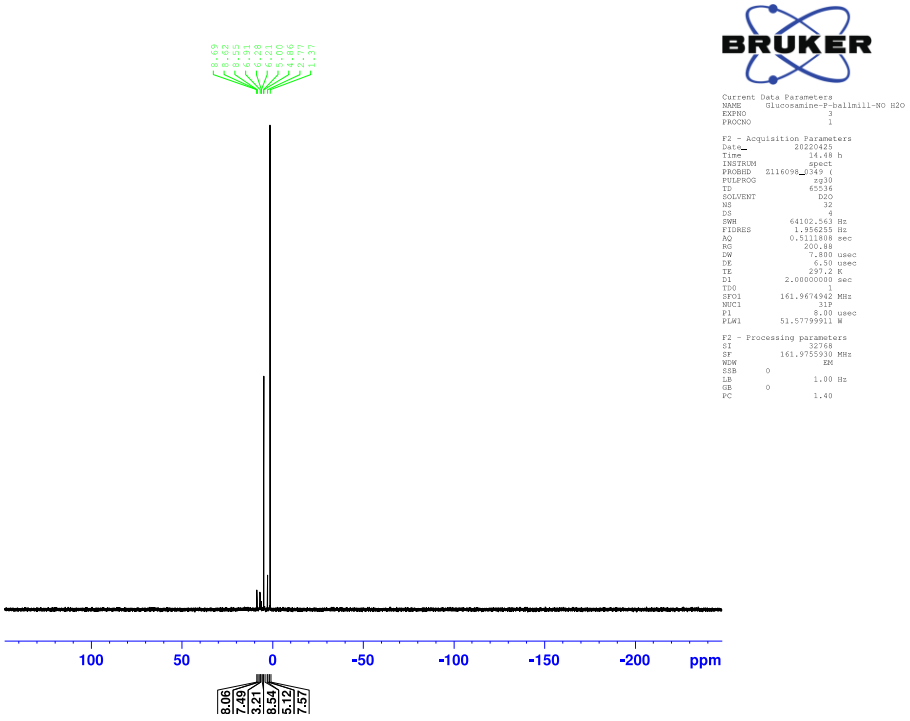

Figure 51: ^{31}P NMR with coupling for glucosamine-P-Ballmill-No H_2O.

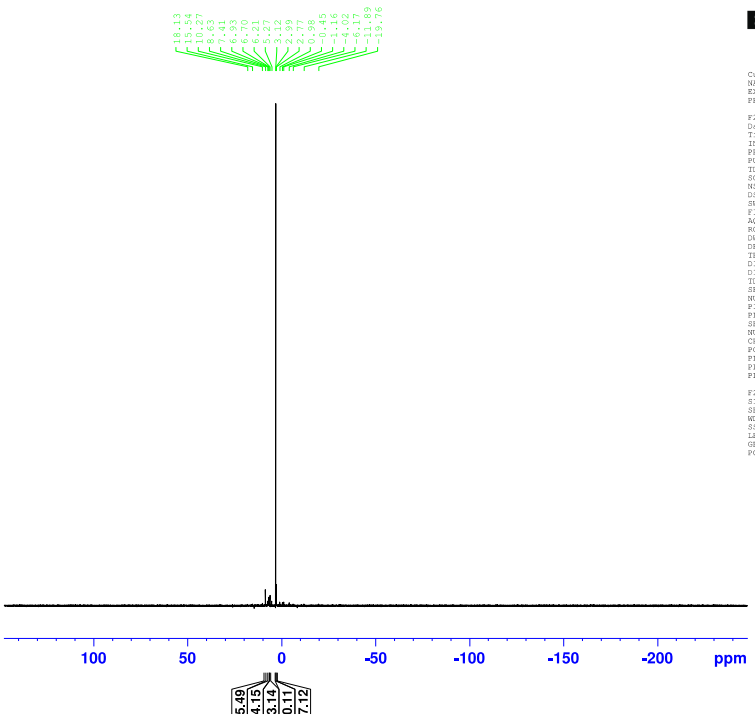

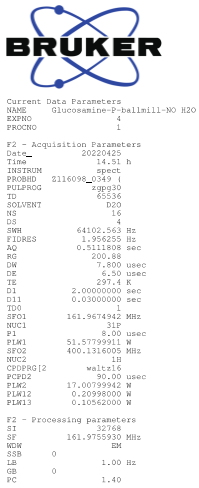

Figure 52: ^{31}P NMR with decoupling for glucosamine-P-Ballmill-No H_2O.